

LEVEL II

12

FLOW RESEARCH COMPANY

A DIVISION OF FLOW INDUSTRIES, INC.

AD A 067902



DDC FILE COPY

DDC
APR 29 1979
C



HEADQUARTERS
21414 - 68th Avenue South
Kent, Washington 98031 (206) 854-1370
Seattle Ex. 622-1500 TWX 910-447-2762

This document has been approved
for public release and sale; its
distribution is unlimited.

79 03 29 026

AD A 067902

DDC FILE COPY

9 Research rept. 12

12 56 p.

Flow Research Report No. 127

6 Numerical Evaluation of Transonic Equivalence Rule

15 NDD 14-76-C-0880

By

10 M. M. Hafez

11 Sept 1978

14 FLOW-RR-127



This document has been approved for public release and sale; its distribution is unlimited.

Flow Research Company
A Division of Flow Industries, Inc.
21414 - 68th Avenue South
Kent, Washington 98031

(206) 854-1370

390 409 Jul
79 03 29 026

Table of Contents

	Page
Summary	iv
1. Introduction	1
2. Transonic Equivalence Rule	4
3. Numerical Models and Numerical Methods	9
4. Numerical Results	14
5. Conclusions	16
Tables	17
Figures	24
References	49

ACCESSION for

NTIS White Section
BDC Buff Section

UNANNOUNCED
JUSTIFICATION *Per the file.*

BY _____
DISTRIBUTION/AVAILABILITY CODES
D. _____ SPECIAL

A

List of Tables

- Table I: Governing Equations.
- Table II: Governing Equation in Inner Region of Transonic Equivalence Rule Formulation.
- Table III: Inner Boundary Condition for Inner Region of Transonic Equivalence Rule Formulation.
- Table IV: Nonlinear Lift Contribution to the Equivalent Body.
- Table V: Transonic Equivalence Rule Formulation, Axisymmetric Limit and Classical 3-Dimensional Wing Theory.
- Table VI: Different Forms of Transonic Small Disturbance Equations.
- Table VII: Modified Transonic Small-Disturbance Equations.

-iii-

List of Figures

- Figure 1. Transonic Flow Field Structure.
- Figure 2. Three-Dimensional Flow Simulation Model With the Second Order Corrections.
- Figure 3. Drag Rise Correlations According to Transonic Equivalence Rule Formulation Based on FFA Experimental Data.
- Figure 4-a. Artificial Compressibility Equation.
- Figure 4-b. Treatment of Regular Points.
- Figure 4-c. Boundary Points.
- Figure 5-a. Sweep Angle Effects.
- Figure 5-b. Drag Rise Characteristics for Wing and its Equivalent Body.
- Figure 5-c. Correlation of Pressure Signatures for Wing and its Equivalent Body.
- Figure 5-d. Correlation of Sonic Lines for Wing and its Equivalent Body.
- Figure 6-a. Lift Correction to Cross-Section Area Distribution.
- Figure 6-b. Sonic Lines of Axisymmetric Flows Around Equivalent Bodies.
- Figure 6-c. Drag Rise for Different Planforms.
- Figure 7-a. Drag Rise Characteristics for Wing and Equivalent Wing Body Combination.
- Figure 7-b. Correlation of Pressure Signatures for Wing and Its Equivalent System.
- Figure 7-c. Correlation of Sonic Lines for Wing and Its Equivalent System.

Numerical Evaluation of Transonic
Equivalence Rule*

Summary

↘ A numerical investigation was conducted to explore the applicability of the transonic equivalence rule. It is shown that for wings of small leading edge sweep angle, departure from Whitcomb-Oswatitsch area rule is significant. For sufficiently large or moderate leading edge sweep-angle, however, the agreement is satisfactory. Drag-rise and outer flow field calculations are presented for a number of cases and their equivalent bodies. Nonlinear lift corrections to the classical area rule are examined. There seems to be a surprisingly good agreement between calculated flows around equivalent wing-body combinations with the same wing planform for cases with appreciable lift. ↗

*This work was supported by the U.S. Office of Naval Research under Contract N00014-76-C-0880.^{now} Partial support of NASA Ames in terms of computer time is also acknowledged and discussion with Professor H. K. Cheng of the University of Southern California is appreciated.

1. Introduction

It is well known that the linearized potential equation breaks down for transonic flows. In 1947 von Karman¹ derived the nonlinear transonic small-disturbance equation (TSDE) describing mixed flows and admitting discontinuous solutions. Heuristically, TSDE can be obtained by replacing the freestream Mach number appearing in the linearized potential equation by the local Mach number. On the other hand, TSDE is an approximation of the full potential equation (where the flow is assumed to be almost parallel to the x-axis, see Table I). If the full potential equation and the exact boundary condition are used, we are left with one single parameter, namely the freestream Mach number M_∞ .

Many three-dimensional flows around practical configurations can be categorized, however, according to geometrical parameters, thickness ratio τ , angle of attack α , and aspect ratio λ .

For example, when the aspect ratio approaches zero we have an axisymmetric flow while two-dimensional flows are obtained in the limit of infinite aspect ratios. There are many interesting asymptotic theories to bridge the gap between the full three-dimensional problem and the above two limits. Starting from the two-dimensional strip theory, lifting line (and yawed lifting line) theories provide corrections for the three-dimensional effects. On the other end, the area rule and the equivalence rule are generally tied with the axisymmetric limit.

In this report, we will examine the validity of the area rule and the equivalence rule and provide a numerical assessment of their range of applicability. The transonic area rule of Whitcomb² and Oswatitsch³ may be stated as follows: At transonic speed, the outer flow far from the configuration is the same as that produced by an (equivalent) body of revolution with the same axial distribution of cross-sectional area. The area rule is based on the assumption of a flow model consisting of two distinct regions, an inner region governed by a Laplace equation, the same as that in the slender body theory, and an outer nonlinear region which is axisymmetric. The above assumption maybe justified for $\alpha = O(\tau)$, $\lambda = O(\tau)$ and $1 - M_\infty^2 = O(\tau^2)$.

Spreiter and Stahara⁴ considered small lift perturbations with the same flow model; an inner region governed by a Laplace equation and an

outer nonlinear axisymmetric region; the only difference is that the inner region here admits a cross flow solution accounting for small lift perturbation to wings of unit order aspect ratios. Hence $\alpha = O(\tau)$, $\lambda = O(1)$ and $1 - M_\infty^2 = O(\tau^2)$.

Recently Cheng and Hafez⁵, and also Barnwell⁶ modified the area rule to account for appreciable lift effects for moderate aspect ratio wings. The lift contributions proves to be essential in the operating ranges of modern aircraft. In their model, the inner region is governed by a second order equation in the velocity potential (cubic terms are neglected), and cast into a Poisson's form (see Table II) where successive approximations involve nonlinear corrections to the slender body theory. The outer region is not axisymmetric and is governed by the three-dimensional classical nonlinear transonic small-disturbance equation. The precise range of the outer region depends on the degree of lift control. The outer flow field structure is determined principally by a line source and a line doublet. The line doublet distribution is proportional to the local lift force (integrated over the wing upstream of the x station) and maybe estimated using the linear theory. The line source strength corresponds to an equivalent body whose cross-sectional area is always bigger than the geometrical cross-sectional area distribution of the wing and the difference depends nonlinearly on the lift distribution. This nonlinear lift contribution to the equivalent body results from the second order corrections to the inner cross flow solution (namely due to the nonhomogeneous terms in the Poisson's equation as well as a second order correction to the inner boundary condition in the cross flow plane) (see Table III). These second order corrections produce accumulative effects of first order importance in the outer flow; and they are not accounted for by the classical transonic small disturbance theory. Roughly the class of three-dimensional transonic flows, where the equivalence rule described above, is applicable, is

$$\alpha = O(\sqrt{\tau/\lambda^3}), \quad \lambda = O(1), \quad 1 - M_\infty^2 = O(\tau\lambda) \quad \text{or} \quad 1 - M_\infty^2 = O(\alpha^2\lambda^4) .$$

A more precise statement of the equivalence rule and its range of validity will be given in Section 2. In Section 3, the modified transonic small-disturbance equation and the second order boundary condition is examined as a model for numerical simulation of transonic flows past thin wings having swept leading edges with smooth lift and thickness distribution. Also, the numerical method employed is briefly discussed. Our numerical results are presented in Section 4.

2. Transonic Equivalence Rule

In the following, x , y and z denote Cartesian coordinates, with the z -axis pointing in the lift direction. Alternately, cylindrical polar coordinates (x , r and ω) are also used. The length scales l and b characterize the axial distribution of the thickness and the half span respectively.

Four parameters λ , τ , α and M_∞ are used to characterize the flow over a wing;

$$\lambda = b/l \quad ,$$

$$\tau = S_{cmax}/b^2 \quad ,$$

$$\alpha = F_{max}/\rho_\infty U_\infty^2 b^2 \quad ,$$

$$M_\infty = U_\infty/a_\infty \quad .$$

The maximum cross-sectional area is denoted by S_{cmax} and the maximum lift is F_{max} . To avoid multiple asymptotic limits, these parameters are replaced by an alternative group of four, ϵ , σ_* , K and Γ_* , where

$$\begin{aligned} \epsilon &= \sqrt{(\gamma + 1) M_\infty^2 \tau \lambda^3} \quad , \\ \sigma_* &= \sqrt{(\gamma + 1) M_\infty^2 |\ln \epsilon| \frac{\alpha^2 \lambda^3}{\tau}} \quad , \\ K &= \frac{1 - M_\infty^2}{(\gamma + 1) M_\infty^2 \tau \lambda} \quad , \\ \Gamma_* &= \frac{8}{\gamma + 1} \frac{1}{|\ln \epsilon| \lambda^2} \quad . \end{aligned}$$

The parameter ϵ is the ratio of the transverse length scale of the inner flow region b , to that of the outer region far from the wing. Essential to the equivalence rule is the existence of a distinct inner region which is small compared with the outer region, thus the formulation is developed for fixed σ_* , Γ_* and K in the single limit

$\epsilon \rightarrow 0$. When ϵ approaches zero, the outer flow sees the body and its vicinity as a line segment along the axis and the presence of the body is felt mainly in the form of a line source and a line doublet.

Inner Region:

The inner flowfield is described basically by the solution of a linear equation (as in the slender body theory),

$$\phi_{yy} + \phi_{zz} = 0 \quad , \quad (1)$$

and the successive approximations with nonlinear corrections as discussed in the introduction of this report. This solution ceases to be valid far from the x-axis. An examination of the non-uniformity of this solution reveals the important parameters and proper scalings for the outer region.

Outer Region:

The inner solution breaks down at a distance of the order b/ϵ from the axis, where the problem is reformulated with reduced variables:

$$\bar{x} = x/\ell \quad , \quad \eta = \epsilon r/b \quad , \quad \bar{\phi} = \frac{\phi}{\tau U_{\infty} b} \quad .$$

The governing equation in the outer region is the familiar three-dimensional transonic small-disturbance equation,

$$(K - \bar{\phi}_{\bar{x}}) \bar{\phi}_{\bar{x}\bar{x}} + \frac{1}{\eta} (\eta \bar{\phi}_{\eta})_{\eta} + \frac{1}{\eta^2} \bar{\phi}_{\omega\omega} = 0 \quad . \quad (2)$$

With the far field condition, $\bar{\phi} \rightarrow 0$ as $\bar{x}^2 + \eta^2 \rightarrow \infty$. In the outer variables (\bar{x} , η and ω), the inner region shrinks to the vicinity of the axis ($\eta = O(\epsilon)$) where Equation (2) admits an expansion for $\eta \ll 1$ in the form:

$$\begin{aligned} \bar{\phi} \sim & D(\bar{x}) \frac{\sin \omega}{\eta} + C_0(\bar{x}) \ln \eta + C_1(\bar{x}) \\ & + \frac{1}{16} (D_{\bar{x}\bar{x}}^2)_{\bar{x}} (21\eta^2 + \cos 2\omega) + \dots \end{aligned} \quad (3)$$

Matching:

Equation (3) permits matching with the inner solution. Subsequently, the doublet strength $D(\bar{x})$ is identified with the lift and the source strength $C_0(\bar{x})$ is identified with the rate of change of the geometrical cross-sectional area distribution of the wing plus nonlinear lift effects. The last term in Equation (3) arises from the nonlinear correction to the slender body Equation (1) and is fixed once the lift distribution is given. A part of the unknowns of the boundary value problem describing the outer flow is $C_1(x)$.

The lengthy analysis of Cheng and Hafez⁵ determines $D(\bar{x})$ and $C_0(\bar{x})$.

$$D(\bar{x}) = \frac{1}{2\pi} \sigma_* |\ln \epsilon|^{-1/2} F(\bar{x}) \quad ,$$

$$C_0(\bar{x}) = \frac{1}{2\pi} S'_e(\bar{x}) \quad . \quad (4)$$

Where $F(\bar{x})$ is a dimensionless lift at \bar{x} and $S_e(\bar{x})$ is normalized by the maximum geometrical cross-sectional area $S_{c \max}$:

$$F(\bar{x}) = \int_{-\infty}^{\infty} \left[\tilde{\phi} \right] dy \quad \text{and} \quad F(1) = 1 \quad ,$$

$$S_e(\bar{x}) = S_c(\bar{x}) + \text{Nonlinear Lift Contribution (See Table IV)}$$

Notice, $\tilde{\phi}$ is the potential jump normalized by αUb ; y and s are normalized by b and it can be shown that the nonlinear lift contribution to the equivalent body is always positive, i.e.,

$$S_e(x) \geq S_c(x) \quad .$$

Cheng⁷ calculated the equivalent body cross-sectional area for different lifting surface arrangements and the nonlinear lift corrections were found to be significant. In summary, the outer region is not axisymmetric, but it is governed by the three-dimensional transonic small-disturbance equation and controlled by a line doublet; its strength proportional to

the lift distribution and a line source corresponding to an increased cross-sectional area distribution depending nonlinearly on the lift. The flow field structure is described in Figure 1. The present formulation complements the classical three-dimensional wing formulation (to which transonic equivalence rule does not apply since $\tau^{1/3}\lambda$ is kept fixed and not small) and reduces to the axisymmetric limit if $\lambda = 0(\tau)$ as seen from Table V.

Drag:

The previous formulation shows that the structure of the outer nonlinear flows around different geometries at a specified transonic parameter K , including the shock and sonic boundaries, is the same, as long as the distributions $S'_e(x)$ and $D(x)$ remain unchanged. Associated with the outer pressure field, is the wave drag D_W which can be correlated as

$$D_W / \rho_\infty U_\infty^2 b^2 \tau^2 M_\infty^2 = f(K) \quad (5)$$

from the entropy increase behind shocks where

$$f(K) = -\frac{1}{12} \iint \left[\frac{\phi}{x} \right]^3 n d\omega d\eta .$$

Equation 5 may also readily be inferred from the form of pressure drag based on the inner solution. For drag rise correlation*, it is assumed that the contribution of the inner region to the shock loss is negligible. For moderate sweep wings, the locally supersonic flow component may support spanwise-running shocks and hence a drag far greater than D_W . If, however, the local flow component remains shock free (e.g., supercritical wing sections), the present theory may be applied to the control of D_W in the outer region.

The total inviscid drag consists of two parts, the wave drag and the induced drag. The induced drag has the same form for transonic as

* Berndt⁹ pointed out that for a nonlifting configuration the drag will be the same as that associated with an equivalent body of revolution provided the configuration ends in a circular constant cylinder or a circular pointed rear body otherwise the correlation involves a term proportional to $S'_c(\ell)$.

for linearized supersonic or subsonic flow and hence, it would be advantageous to have an elliptical spanwise lift distribution provided that the wave drag is not unduly increased (see Cole⁸).

Recently, the validity of transonic similarity rule and transonic area rule for wing-body combinations with fairly thick moderately swept tapered wings of intermediate aspect ratios has been experimentally explored at FFA¹⁰. The motivation was that wings with supercritical airfoils designed by computational methods for two-dimensional flow has been wind tunnel tested, but the improvement in drag characteristics demonstrated in two-dimensional tests, did not come out in three-dimensional tests. It was obvious that more detailed insight had to be gained about three-dimensional transonic flow field structure around swept wings of moderate aspect ratios. The most important aerodynamic concept in this regard is, perhaps, the transonic area rule. In short, to control the drag in the neighborhood of the wing, a good design of the wing section is necessary, at the same time, to control the drag due to shocks extending in the outer and far field, the three-dimensional assembly of these wing sections plays a critical role; the equivalence rule provides the tools to control these three-dimensional aspects of the problem namely through the equivalent line source and line doublet distributions. Of interest here is their experimental results for the transonic similitude. According to the present theory, the general correlation of drag rise, given by:

$$\frac{\Delta C_{Dw}}{\tau^{5/3}} = f(K, \tau^{1/3}\lambda, \frac{\alpha}{\tau}) ,$$

reduces to

$$\frac{\Delta C_{Dw}}{\tau^{5/3}} = M_\infty^2 \tau^{1/3}\lambda f(K) ,$$

where ΔC_{Dw} is based on the wing area.

We used the FFA experimental data for three affinely related wings to examine our drag rise correlation formula. Their results are plotted in Figure 3 where indeed $f(K)$ versus K relationship reduces to a single curve for the three wings.

3. Numerical Models and Numerical Methods

In this section, the complete three-dimensional flow simulation model will be examined. Also, flow simulation around equivalent source and equivalent doublet distributions will be considered.

As discussed before, second order corrections to the transonic small-disturbance equation and to the wing boundary condition produces first order effects in the outer flow which are not accounted for by the classical theory. The modified boundary value problem is described in Figure 2. The numerical solution is needed to assess the present asymptotic theory and to verify the flow field structure described earlier in Figure 1. The complete three-dimensional problem involves two length scales (the inner and the outer regions), and in addition, all the details of the shape of the wing must be considered. On the other hand, the equivalent system completely avoids the geometrical complexity and describes only the outer region. For small lift perturbation, the equivalent system can be further simplified to an axisymmetric flow around a line source plus a lift perturbation governed by an axisymmetric equation. Of interest is the perturbation of the shock as discussed in Reference 11. For cases with appreciable lift the second order nonlinear effects are important and these effects appear in the feedback term as well as in the strength of the equivalent line source.

Review of Existing Numerical Models for Three-Dimensional Transonic Flows

At present, approximate transonic flow calculations can be performed for arbitrary lifting wings and moderately complicated wing-fuselage combinations using relaxation type-dependent finite difference techniques. Most methods are based on transonic small perturbation theory, but different model equations are used.

The classical von Karman-Cole equation is derived with the assumptions:

$$\phi = O(\tau^{2/3}),$$

$$1 - M_\infty^2 = O(\tau^{2/3})$$

and y, z are scaled to $(\tau^{1/3})$, where τ is the thickness ratio. Different forms of transonic small-disturbance equations are given in Table VI.

A deficiency in the treatment of wings with moderate to large sweep angles leads Lomax, Bailey & Ballhaus¹² to appeal to higher order terms in order to obtain better approximation of the full potential equation in regions of the flow field that are essentially two-dimensional in a plane normal to the sweep direction. Hence, a modified equation (including two extra terms in order to satisfy two-dimensional sweep theory) is introduced.

Newman & Klunker¹³ modified the classical equation in another way. An extra term is added for a better approximation of the critical speed where the equation changes type, from elliptic to hyperbolic.

Recently, van der Vooren et al.¹⁴ introduced another modified equation. In their work, other models are criticized for not being a proper small perturbation of the mass conservation law. Starting from the full potential equation in conservative form, a new transonic small perturbation equation is derived. They rederived the Lomax-Bailey-Ballhaus equation along this line. The resulting equation is different from Lomax's equation (written in conservative form) only by third order terms for smooth flow. Their shock relations, however, differ significantly.

Other authors resort to the empirical formula of the transonic similarity parameter and pressure coefficient to obtain good results.

The different models of the modified transonic small-disturbance equation are given in Table VII.

Present Model

The existing models are not adequate for the equivalence rule calculations since the $(\phi_z^2)_x$ term is neglected. For the class of configuration of interest here, $(\phi_z^2)_x$ term is of the same order as $(\phi_y^2)_x$. In the present analysis, the oblique shock is avoided by using, for example, supercritical wing sections. Nevertheless the second order terms are retained to allow for their accumulative effects in the outer region.

The complete formal second order equation is obtained first. The governing equation is written in the conservation form:

$$\left(\rho(1 + \phi_x)\right)_x + (\rho\phi_y)_y + (\rho\phi_z)_z = 0 \quad (6)$$

where ρ is a unique function of the velocity. Different expressions for ρ are used namely,

(I) The full potential equation:

$$\rho = \left(1 - \frac{\gamma - 1}{2} M_\infty^2 ((\phi_x + 1)^2 + \phi_y^2 + \phi_z^2 - 1)\right)^{\frac{1}{\gamma - 1}} \quad (7)$$

(II) The second order modified small-disturbance equation:

$$\begin{aligned} \rho = 1 - \frac{1}{2} M_\infty^2 (\phi_x^2 + 2\phi_x + \phi_y^2 + \phi_z^2) \\ + \frac{2 - \gamma}{2} M_\infty^4 (\phi_x^2 + \phi_x^3) - \frac{2 - \gamma}{6} (3 - 2\gamma) M_\infty^6 \phi_x^3 \quad (8) \end{aligned}$$

(III) The transonic small-disturbance equation:

$$\rho = 1 - \frac{1}{2} M_\infty^2 (2\phi_x + \phi_x^2) + \frac{2 - \gamma}{2} M_\infty^4 \phi_x^2 \quad (9)$$

The shock relations in each case are consistent with the perturbation of the Rankine-Hugoniot relation since the corresponding governing equation is a proper perturbation of the mass conservation.

Following Schmidt¹⁵, mass should also be conserved across the boundaries. The consistent boundary conditions for the above cases are given as follows:

(I) Exact boundary condition:

$$\rho(1 + \phi_x) B_x + \rho\phi_y B_y + \rho(\phi_z + \alpha) B_z = 0$$

$$\text{on } B(x, y, z) = 0 \quad (10)$$

(II) Second order boundary condition:

$$\begin{aligned} \rho(\alpha + \phi_z) \Big|_0 &= \left[\rho(\phi_z + \alpha) - (\rho\phi_z)_z \quad z \right]_W \\ &= \left[(\rho(1 + \phi_x))W_x + (\rho\phi_y)W_y + z(\rho(1 + \phi_x))_x \right. \\ &\quad \left. + z(\rho\phi_y)_y \right]_W \\ &= \left[(\rho(1 + \phi_x) \cdot W)_x + (\rho\phi_y \cdot W)_y \right]_W \end{aligned} \quad (11)$$

where $z = W(x,y)$ describes the wing geometry.

(III) Conservative boundary condition for the transonic small-disturbance equation:

$$\rho(\alpha + \phi_z) = \rho(1 + \phi_x) W_x \quad \text{on } z = 0 \quad . \quad (12)$$

Equation 12 was used by Schmidt¹⁵ in two-dimensional calculations instead of the linearized boundary condition:

$$\phi_z = W_x - \alpha$$

Where he obtained better agreement with the full potential solution.

Numerical Treatment of Modified Second Order Equation

Ballhaus and Baily and also van der Vooren et al.¹⁴ used the rotated difference scheme (originally developed by Jameson for the full potential equation¹⁶). South²⁰ discussed some of the difficulties encountered in the solution of three-dimensional modified small-disturbance equations (diagonal dominance versus conservative forms).

Recently, a new method was developed for the numerical solution of the full potential equation. Using an artificial density (with extra terms due to the artificial viscosity), standard discretization techniques (centered differencing everywhere) and standard iterative procedures

(SOR, ADI, Explicit Method) are shown to be applicable to the nonlinear full potential equation written in conservation form. The mixed type equation is treated as if it were elliptic with the density evaluated from previous iteration. Two-dimensional results are reported in Reference 17. This method is briefly described in Figure 4.

The artificial compressibility method is adopted here. A code is developed to solve the three-dimensional problem using cylindrical polar coordinates. With the same code, the full potential equation, the modified second order equation or the transonic small-disturbance equation is solved depending on the expression for the density in terms of the velocity. The equation is always in conservation form. Consistent boundary conditions conserving mass are implemented in a straight forward manner. The results obtained in this report are based on a standard successive over-relaxation procedure applied to the modified second order equation. The outer boundary condition can be chosen according to a far field formula (similar to Klunker's) or simply ϕ vanishes or ϕ_r vanishes (solid wall tunnel).

4. Numerical Results

We calculated three-dimensional flows around trapezoidal wings with NACA four digit sections, mounted on a cylinder for zero- and 2° -angle of attack at Mach number ranges (0.94 to 0.97). The leading edge sweep angles are 30° , 45° and 60° . The trailing edge sweep angle is always 15° .

The numerical details will not be discussed here. Only preliminary results in terms of the drag rise and the flow field pressure signature will be reported.

Transonic Area Rule at Zero Lift

The wave drag of different wings at zero lift and their equivalent body of revolutions are calculated. The results are plotted in Figure 5-a. For a 60° -swept wing, the difference in the drag of the wing and its equivalent body of revolution is 2 percent, while for a 45° -wing the difference is 12 percent and for a 30° -wing, the difference is 46 percent. In all these cases, there is only one shock on the wing.

In Figure 5-b, the drag rise characteristics for the 30° -wing and its equivalent body are shown. The significant deviation from the area rule may be attributed to the different behavior of the shock in the inner region. The wing carries a stronger shock than the body of revolution and the contributions of the inner regions to the drag are neither negligible nor the same. The outer flow fields correlation is shown in Figures 5-c and 5-d.

Lifting Area Rule

In an attempt to simplify the equivalence rule formulation, Barnwell¹⁸ restricted the lift effect to the equivalent source strength and calculated an axisymmetric flow around a body of revolution.* Comparisons of wing-plane results for lifting and equivalent axisymmetric flow indicate the applicability of this engineering approach. Sedin¹⁹ presented similar calculations of the transonic drag-rise due to lift only and showed good quantitative agreement with experimental data.

*Barnwell also allowed for full three-dimensional effects, where an approximation for the deviation from the axisymmetric flow is evaluated analytically and a two-variable problem is computed for each azimuthal plane.

Obviously, this is a partial account for the lift effects. The line doublet which is linearly proportional to the lift distribution as well as the nonlinear lift contribution to the feedback term will introduce asymmetry to the outer region. As pointed out by Cheng and Hafez⁵, however, the equivalent line source is asymptotically stronger than the line doublet as well as the feedback term by a factor of $1/\ln \epsilon^{1/2}$, hence the outer flow becomes axisymmetric in the strict asymptotic limit even for a wing without thickness ($\sigma_* \rightarrow \infty$).

Equivalent body cross-sectional areas of Mach 0.98 design with four alternative lifting-surface arrangements were studied by Cheng⁷. Here axisymmetric flows around these equivalent bodies are calculated. The sonic line and wave drag for each case are shown in Figure 6.

Transonic Equivalence Rule

Here the asymmetrical effects due to lift will be considered. Three-dimensional flows around a wing of 30° -sweep leading edge at 2° -angle of attack and different Mach numbers are calculated. The equivalent system is another complete three-dimensional flow around a wing-body combination; the wing has zero thickness, but the same plane form and the body has the same cross-sectional area distribution as the original wing.

Although the inner regions are different for the two configurations, their outer limit is the same, i.e., the equivalent source and the equivalent doublet are the same for the wing and the wing body combination. Hence, according to the present theory the drag rise characteristics are the same. The results of the calculations are plotted in Figure 7-a and show good agreement between the two cases. The pressure signature in the inner- and outer flow fields are presented in Figure 7-b. Needless to say, this single example checks only the concept, but not the formulation. More numerical results are needed to support the theory.

5. Conclusions

The transonic area rule and the necessary modifications due to lift are examined. The numerical results indicate good agreement of drag rise characteristics for large swept wings and their equivalent bodies of revolution. The departure is significant for wings of small leading edge sweep angle. The flow field far from the wing is axisymmetric and correlates with that around the equivalent body of revolution, the shock losses in regions near the wing and near the body are different and not negligible.

The increase in the cross-sectional area distribution of the equivalent body of revolution due to nonlinear lift effects leads to significantly different wave drag. The modified area rule can be indeed a useful tool to examine the three-dimensional aspects of different designs at least qualitatively. Quantitative agreements, however, are shown for calculated flows around different wing body combinations with the same wing plan form and the same total geometrical cross-sectional area distribution for cases with lift. More examples are needed to support both the concept and the formulation of the present theory.

Tables

Second Order Potential Perturbation Equation:

$$(1 - M^2) \phi_{xx} + \phi_{yy} + \phi_{zz} = M_\infty^2 (\phi_y^2 + \phi_z^2)_x + \text{cubic terms}$$

where

$$1 - M^2 \approx 1 - M_\infty^2 + (\gamma + 1) M_\infty^2 \phi_x$$

Laplace Equation in the Cross Flow Plane:

$$\phi_{yy} + \phi_{zz} = 0$$

Poisson's Equation in the Cross Flow Plane:

$$\phi_{yy} + \phi_{zz} = (M^2 - 1) \phi_{xx} + M_\infty^2 (\phi_y^2 + \phi_z^2)_x$$

Table II. Governing Equation in Inner Region of Transonic Equivalence Rule Formulation.

Exact Boundary Condition (Impermeability Requirement):

$$\phi_z = (1 + \phi_x)W_x + \phi_y W_y \quad \text{on } z = W(x,y) \quad .$$

Linearized Boundary Condition:

$$\phi_z = W_x \quad \text{on } z = 0 \quad .$$

Second Order Boundary Condition:

Using Taylor Series Expansion or analytic continuation of the flow from the wing surface to $z = 0$ plane:

$$\begin{aligned} (\phi_z)_0 &= (\phi_z - z\phi_{zz} + \dots)_W \\ &= ((1 + \phi_x)W_x + \phi_y W_y + z(1 - M_\infty^2)\phi_{xx} + z\phi_{yy})_W \quad . \end{aligned}$$

Table III. Inner Boundary Condition for Inner Region of Transonic Equivalence Rule Formulation.

$$\text{Nonlinear Lift Contribution to Equivalent Source} \equiv \alpha_*^2 \left[\left(1 + \frac{1}{2} |\ln \epsilon|^{-1}\right) F \frac{2}{x} + \frac{1}{2} |\ln \epsilon|^{-1} T(\bar{x}) + \frac{1}{8} \Gamma_* E(\bar{x}) \right]$$

where

$$T(\bar{x}) = \frac{1}{4\pi} \int_{a_1}^{a_2} \int_{a_1}^{a_2} \left[\tilde{\phi}(x,s) \right]_x \left[\tilde{\phi}(x,y) \right]_x \ln \frac{1}{|y-s|} ds dy$$

$$E(\bar{x}) = \frac{1}{4\pi} \int_{a_1}^{a_2} \int_{a_1}^{a_2} \left[\tilde{\phi}(x,s) \right]_s \left[\tilde{\phi}(x,y) \right]_y \ln \frac{1}{|y-s|} ds dy$$

a_1 , a_2 are the spanwise ordinates (divided by half span b)

Table IV. Nonlinear Lift Contribution to the Equivalent Body.

Axisymmetric Limit	Transonic Equivalence Rule Formulation (Outer Region)	Classical Three-Dimensional Wing Formulation
$\bar{x} = x/\ell$ $\bar{r} = r/\ell$	$\bar{x} = x/\ell$ $\eta \approx \sqrt{\tau\lambda} \ r/\ell$	$\bar{x} = x/\ell$ $\bar{y} = \tau^{1/3} \ y/\ell$ $\bar{z} = \tau^{1/3} \ z/\ell$
$\phi = \phi/\tau^2 U\ell$ $K = \frac{1 - M_\infty^2}{(\gamma + 1)M_\infty^2 \tau^2}$	$\bar{\phi} = \phi/\tau\lambda \ U\ell$ $K = \frac{1 - M_\infty^2}{(\gamma + 1)M_\infty^2 \tau\lambda}$	$\bar{\phi} = \phi/\tau^{2/3} \ U\ell$ $K_1 = \frac{1 - M_\infty^2}{(\gamma + 1)M_\infty^2 \tau^{2/3}}$
$\epsilon = \tau^2$ $\alpha = 0$	$\epsilon \approx \sqrt[3]{\tau\lambda} \rightarrow 0$ $\sigma^* \approx \sqrt{\frac{2\lambda^3}{\tau}}$	$K_2 = \tau^{1/3} \lambda$ $\frac{\alpha}{\tau}$
Differential Equation: Axisymmetric Boundary Condition: Body of Revolution	3-Dimensional Line Source S_e + Line Doublet D + Feedback Terms (D)	3-Dimensional $\phi_x = W_x(x,y)$ on $z = 0$ + Kutta Condition
$C_p = -2\tau^2 \frac{\bar{\phi}}{x}$ $\frac{D}{\rho_\infty U_\infty^2 \ell^2} = \tau^4 f(K)$	$C_p = 2\tau\lambda \frac{\bar{\phi}}{x}$ $\frac{D}{\rho_\infty U_\infty^2 \ell^2} = M_\infty^2 \tau^2 f(K)$	$C_p = 2\tau^{2/3} \frac{\bar{\phi}}{x}$ $\frac{D}{\rho_\infty U_\infty^2 \ell^2} = \tau^{4/3} f(K_1, K_2, \frac{\alpha}{\tau})$

Table V. Transonic Equivalence Rule Formulation, Axisymmetric Limit and Classical 3-Dimensional Wing Theory.

$((1 - M_\infty^2) + \Gamma \phi_x) \phi_{xx} + \phi_{yy} + \phi_{zz} = 0$	
von Karman	$\Gamma_{vk} = \gamma + 1$
Spreiter	$\Gamma_s = (\gamma + 1) M_\infty^2$
Hayes	$\Gamma_H = (\gamma + 1) M_\infty^4$
Murman & Krupp	$\Gamma_{MK} = (\gamma + 1) M_\infty^{3/2}$
Baily & Ballhaus	$\Gamma_{BB} = (\gamma + 1) M_\infty^{1.558}$
Sirovich & Huo	$\Gamma_{SH} = \frac{(2\gamma+1)M_\infty^2+1}{2}$

Table VI. Different Forms of Transonic Small Disturbance Equations.

<p>Lomax Bailey Ballhaus and Ballhaus Bailey</p>	$\left[(1 - M_\infty^2) \phi_x - \frac{\gamma+1}{2} M_\infty^n \phi_x^2 + \frac{1}{2} (\gamma - 3) M_\infty^p \phi_y^2 \right] x$ $+ \left[\phi_y - (\gamma - 1) M_\infty^p \phi_x \phi_y \right] y + (\phi_z)_z = 0$ <p>n = 1.75, p = 2; n = 1.558, p = 0.162; ...</p>
<p>Newman and Klunker</p>	$\left[(1 - M_\infty^2) - (\gamma + 1) M_\infty^2 \phi_x - \frac{1}{2} (\gamma + 1) M_\infty^2 \phi_x^2 \right] \phi_{xx} + \phi_{yy} + \phi_{zz} = 0$
<p>Schmidt and Vanino</p>	$\left[(1 - M_\infty^2) - (\gamma + 1) \epsilon M_\infty^2 \phi_x \right] \phi_{xx} + \phi_{yy} + \phi_{zz} = 0$
<p>van der Vooren et al.</p>	$\left[1 + (1 - M_\infty^2) \phi_x - \frac{1}{2} (3 - (2 - \gamma) M_\infty^2) M_\infty^2 \phi_x^2 - \frac{1}{2} M_\infty^2 \phi_y^2 - \frac{1}{2} M_\infty^2 \phi_z^2 \right] x$ $+ \left[\phi_y - M_\infty^2 \phi_x \phi_y \right] y + \left[\phi_z - M_\infty^2 \phi_x \phi_z \right] z = 0$
<p>van der Vooren rederivation of Lomax et al. equation</p>	$\left[(1 - M_\infty^2) \phi_x - \frac{1}{2} (3 - (2 - \gamma) M_\infty^2) M_\infty^2 \phi_x^2 - \frac{1}{2} M_\infty^2 \phi_x^2 \right] x$ $+ \left[\phi_y - M_\infty^2 \phi_x \phi_y \right] y + \left[\phi_z \right] z = 0$
<p>Albane, Bass and Joyce</p>	$\left[(1 - M_\infty^2) - (\gamma + 1) M_\infty^2 \phi_x \right] \phi_{xx} + \phi_{xx} + \phi_{xx} - 2\phi_y \phi_{xy} - 2\phi_x \phi_{xz} = 0$

Table VII. Modified Transonic Small-Disturbance Equations.

Far Field:

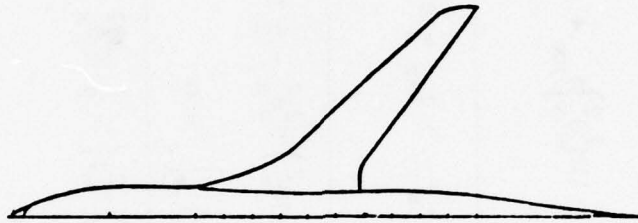
$$\bar{\phi} \approx \frac{S_\infty}{4\pi R} + \frac{E\bar{x}}{4\pi R^3} + \frac{\sin \omega}{2\eta} \left(1 + \frac{x}{R}\right) D_\infty + \frac{K\eta \sin \omega}{2R^3} \int_0^x (D(x) - D_\infty) dx .$$

Outer Region:

$$\left(K = \bar{\phi}_{\bar{x}} \right) \bar{\phi}_{\bar{x}\bar{x}} + \frac{1}{\eta} (\eta \bar{\phi}_{\eta})_{\eta} + \frac{1}{\eta^2} \bar{\phi}_{\omega\omega} = 0 .$$

Inner Region:

$$\bar{\phi} \approx \frac{S'_e(\bar{x})}{2\pi} \ln \eta + D(x) \frac{\sin \omega}{\eta} + \frac{1}{16} \left(\frac{D_{\bar{x}}}{x} \right)^2 (2 \ln^2 \eta + \cos 2\omega) + C_1(\bar{x}) .$$



Far Field Terms:

$$\frac{S_\infty}{4\pi R} \equiv \text{Three-dimensional Source} , \quad R^2 = \bar{x}^2 + K\eta^2 ,$$

$$\frac{E\bar{x}}{4\pi R^3} \equiv \text{Three-dimensional Doublet} ,$$

$$\frac{\sin \omega}{2\eta} \left(1 + \frac{x}{R}\right) D_\infty + \frac{K\eta \sin \omega}{2R^3} \int_0^x (D(x) - D_\infty) dx \equiv \text{horse shoe vortex} .$$

Inner Limit Terms:

$$\frac{S'_e(\bar{x})}{2\pi} \ln \eta \equiv \text{Two-dimensional Source in Cross Flow Plane} ,$$

$$\frac{D(x) \sin \omega}{\eta} \equiv \text{Two-dimensional Doublet in Cross Flow Plane}$$

+ Feedback Terms Due to Nonlinear Corrections.

Figure. 1 Transonic Flow Field Structure.

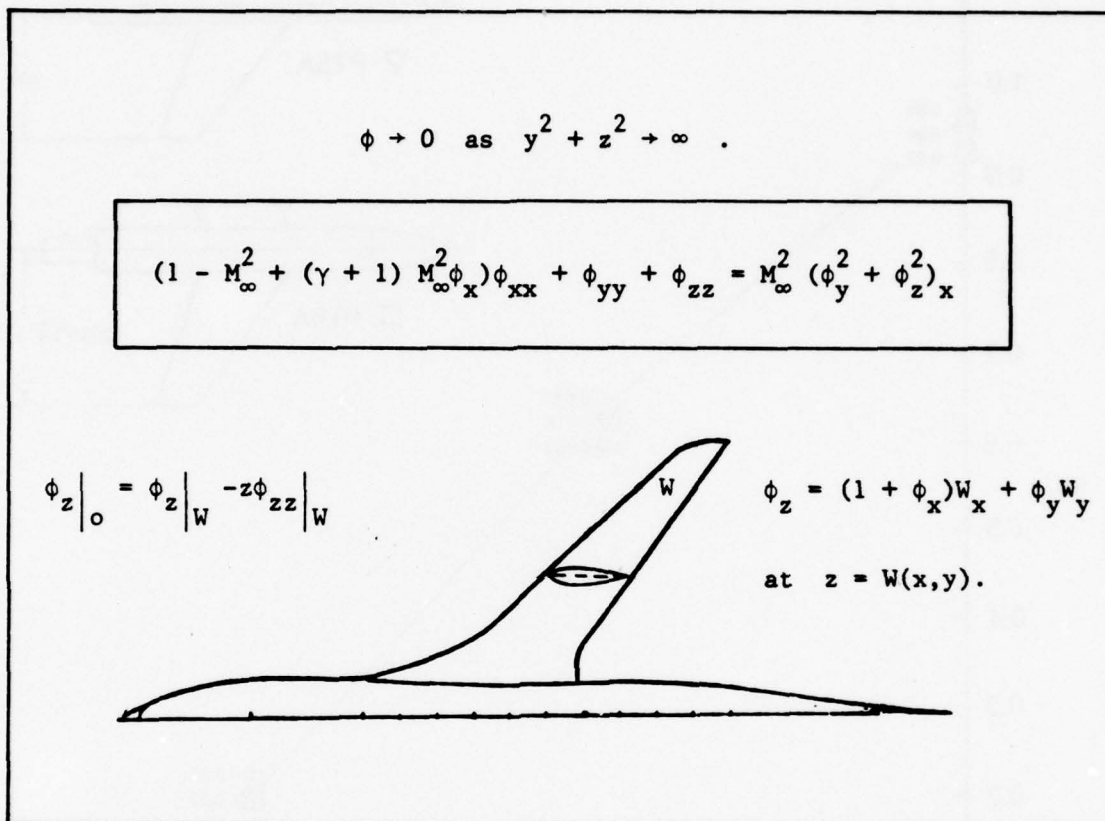


Figure 2. Three-Dimensional Flow Simulation Model With the Second Order Corrections.

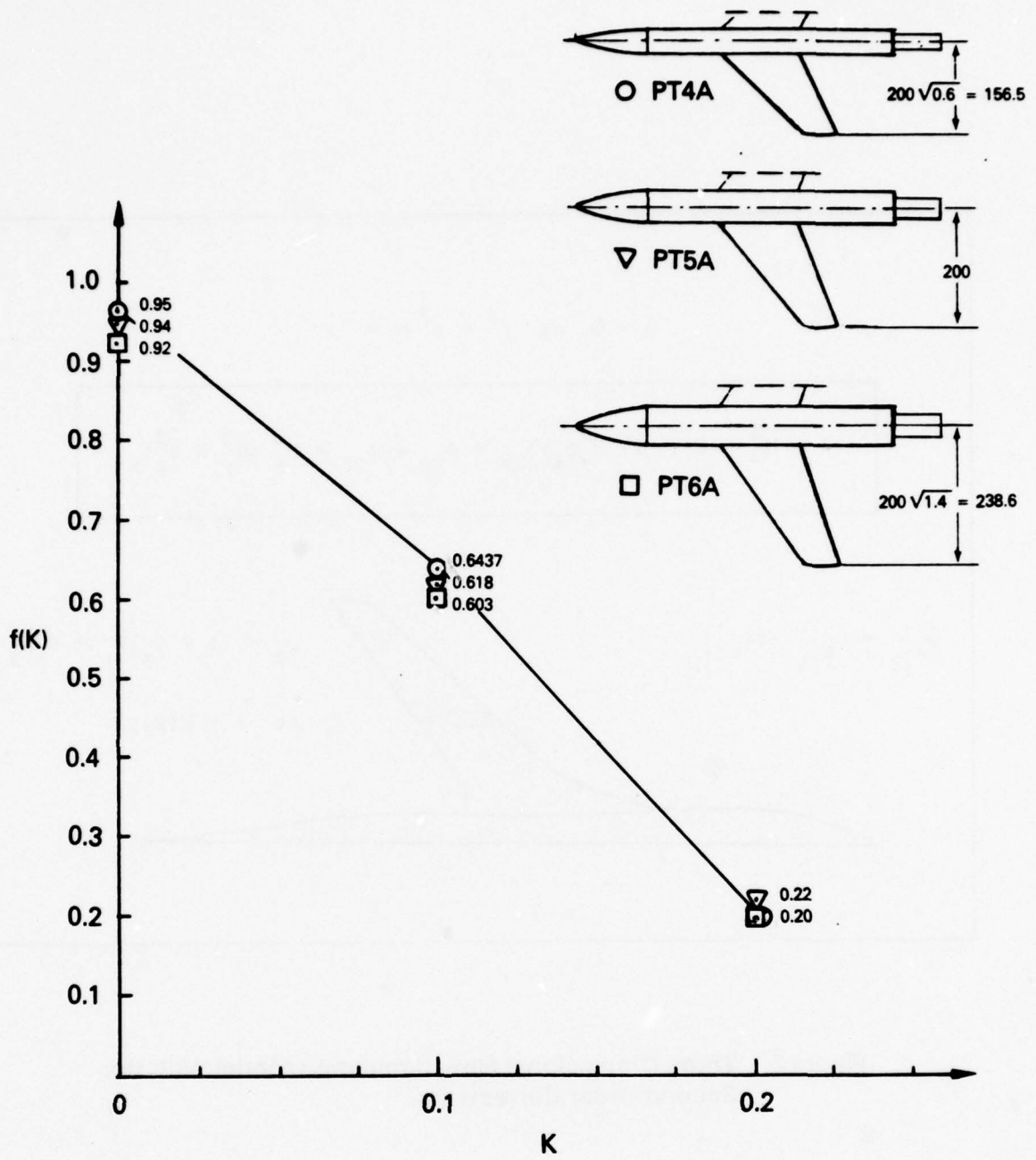


Figure 3. Drag Rise Correlations According to Transonic Equivalence Rule Formulation Based on FFA Experimental Data.

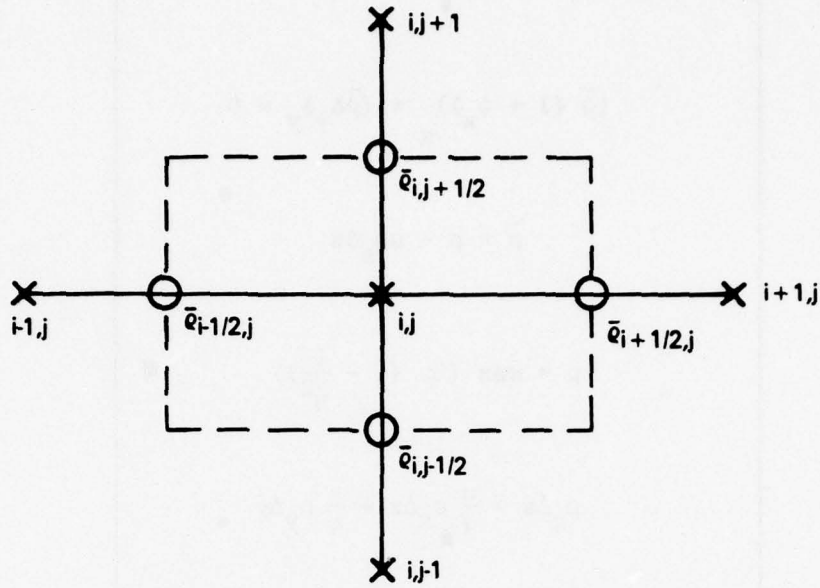
$$(\bar{\rho} (1 + \phi_x))_x + (\bar{\rho} \phi_y)_y = 0$$

$$\bar{\rho} = \rho - \mu \rho_s \Delta s$$

$$\mu = \max (0, (1 - \frac{1}{M^2}))$$

$$\rho_s \Delta s \approx \frac{u}{q} \rho_x \Delta x + \frac{v}{q} \rho_y \Delta y$$

Figure 4-a. Artificial Compressibility Equation.



$$\frac{1}{\Delta y} \left(\bar{\rho}_{i,j+\frac{1}{2}} \frac{(\phi_{j+1} - \phi_j)}{\Delta y} - \bar{\rho}_{i,j-\frac{1}{2}} \frac{(\phi_j - \phi_{j-1})}{\Delta y} \right) + \frac{1}{\Delta x} \left(\bar{\rho}_{i+\frac{1}{2},j} \frac{(\phi_{i+1} - \phi_i)}{\Delta x} + 1 - \bar{\rho}_{i-\frac{1}{2},j} \frac{(\phi_i - \phi_{i-1})}{\Delta x} + 1 \right) = 0 ,$$

$$\bar{\rho}_{i,j+\frac{1}{2}} = (\bar{\rho}_{i,j+1} + \bar{\rho}_{i,j})/2$$

$$\bar{\rho}_{i-\frac{1}{2},j} = (\bar{\rho}_{i+1,j} + \bar{\rho}_{i,j})/2 .$$

Figure 4-b. Treatment of Regular Points.

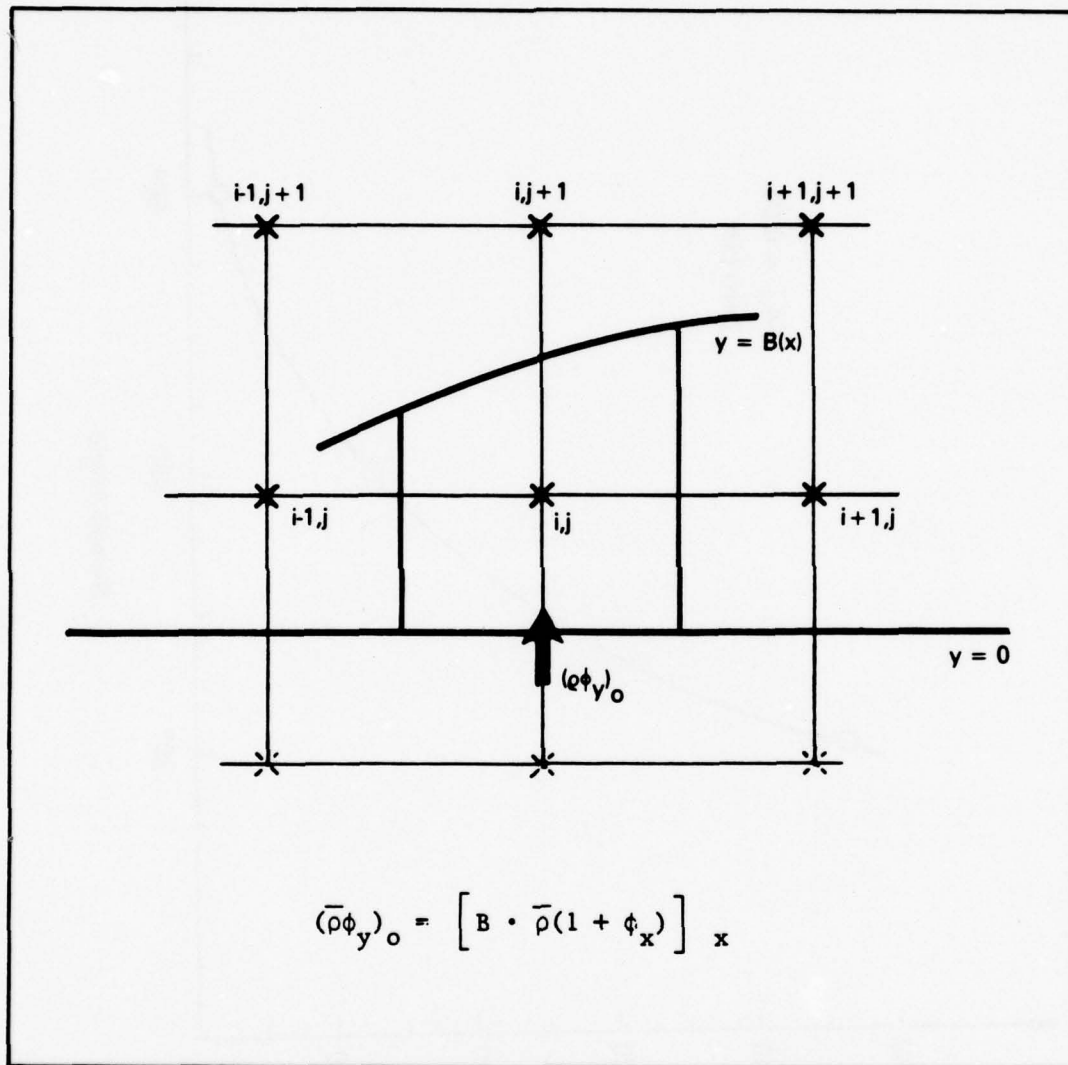
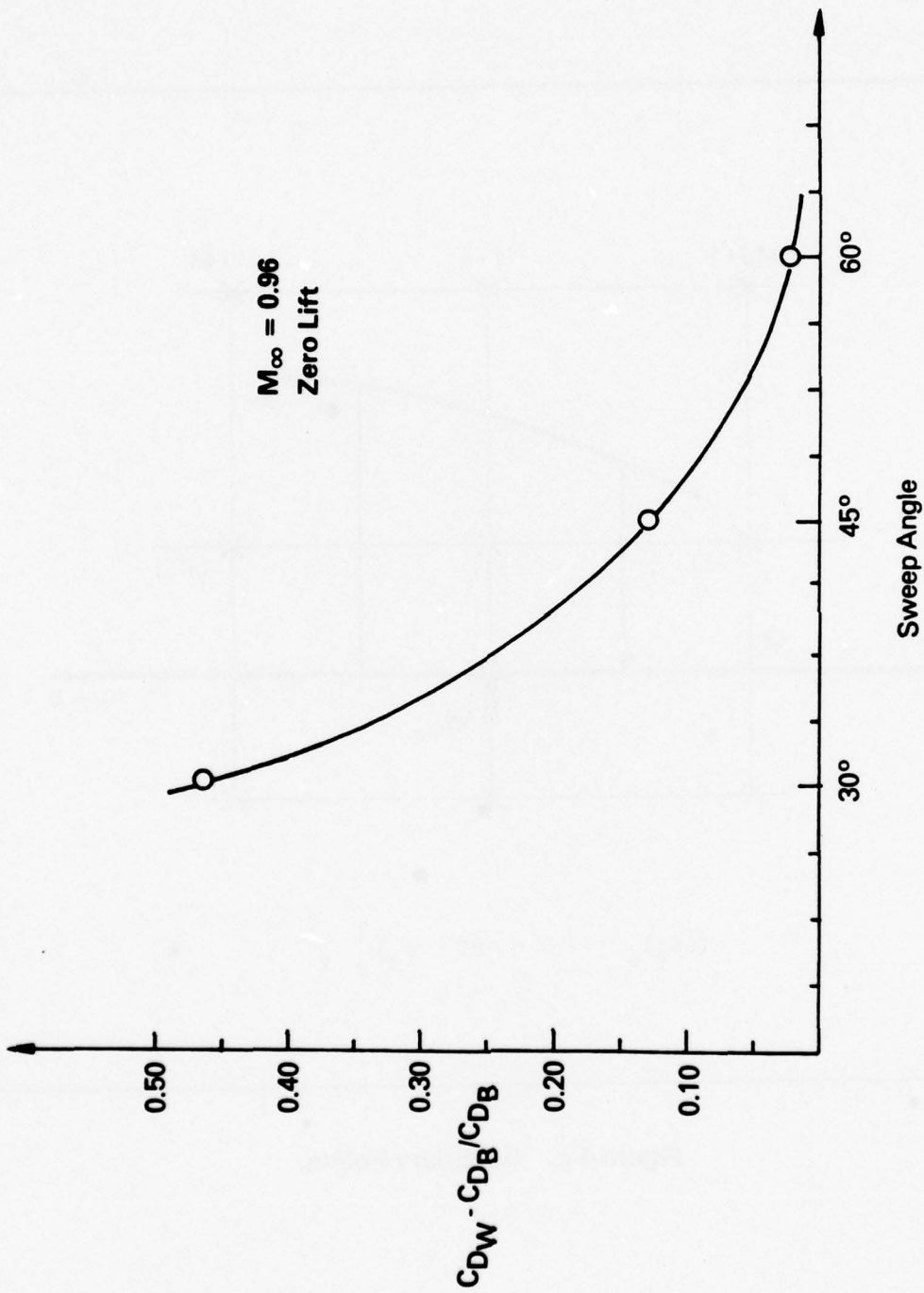


Figure 4-c. Boundary Points.



$M_{\infty} = 0.96$
Zero Lift

Figure 5-a Sweep Angle Effects.

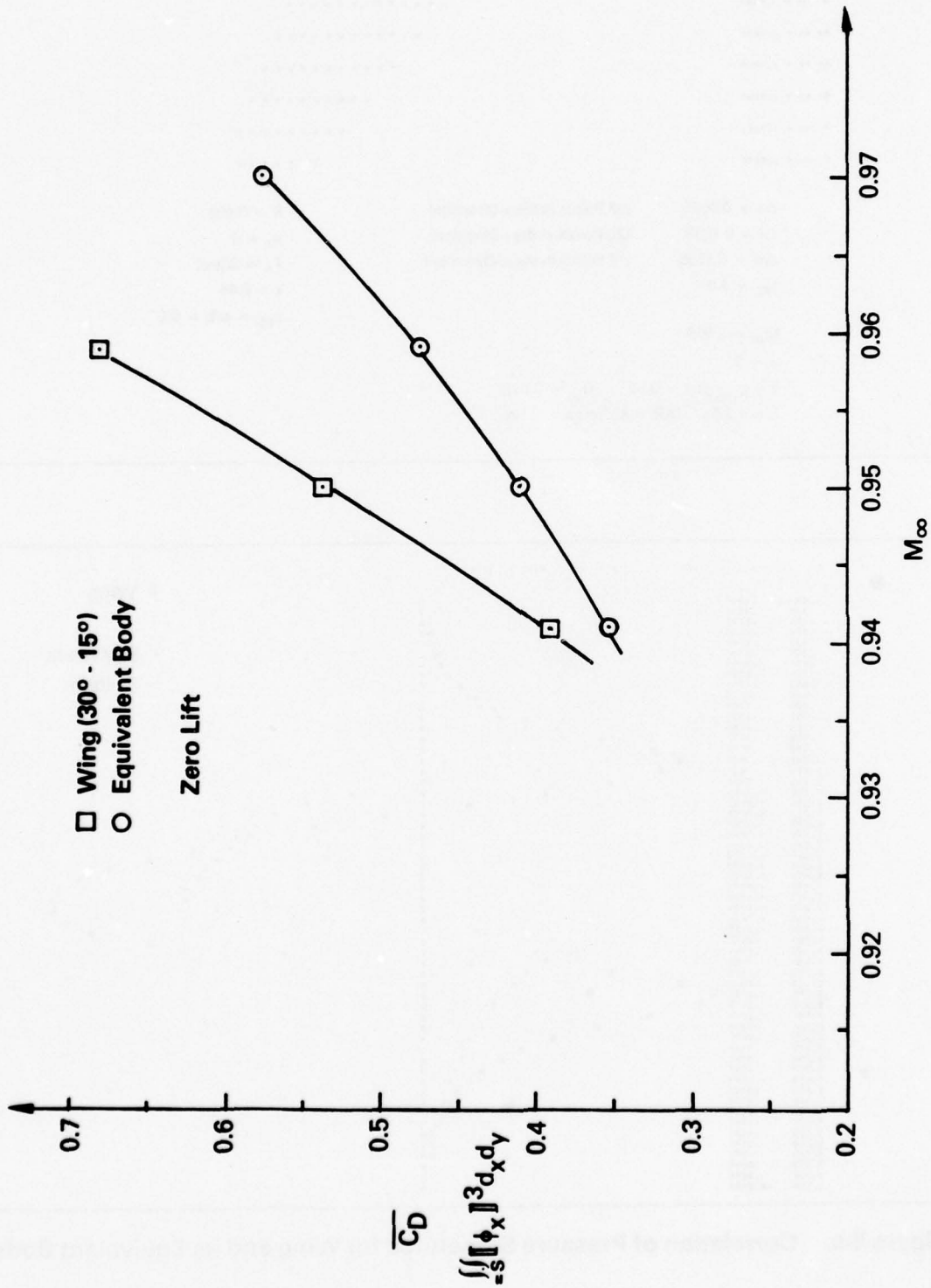


Figure 5-b. Drag Rise Characteristics for Wing and its Equivalent Body.

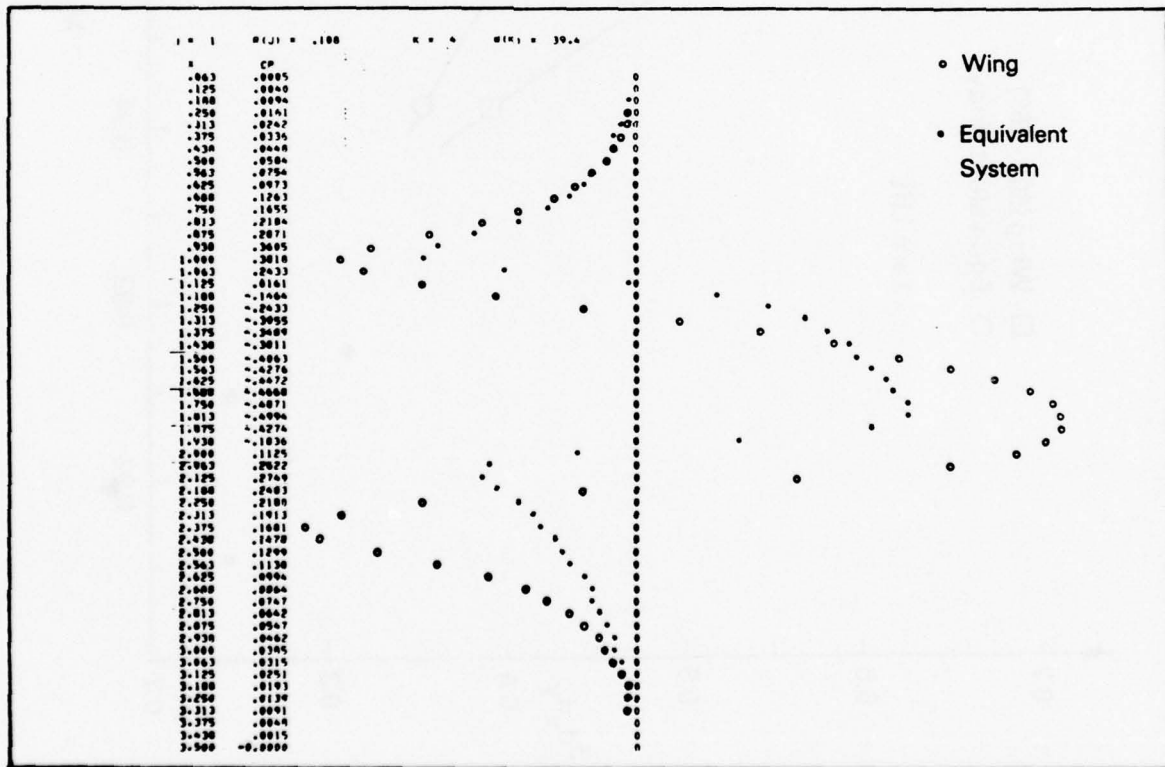
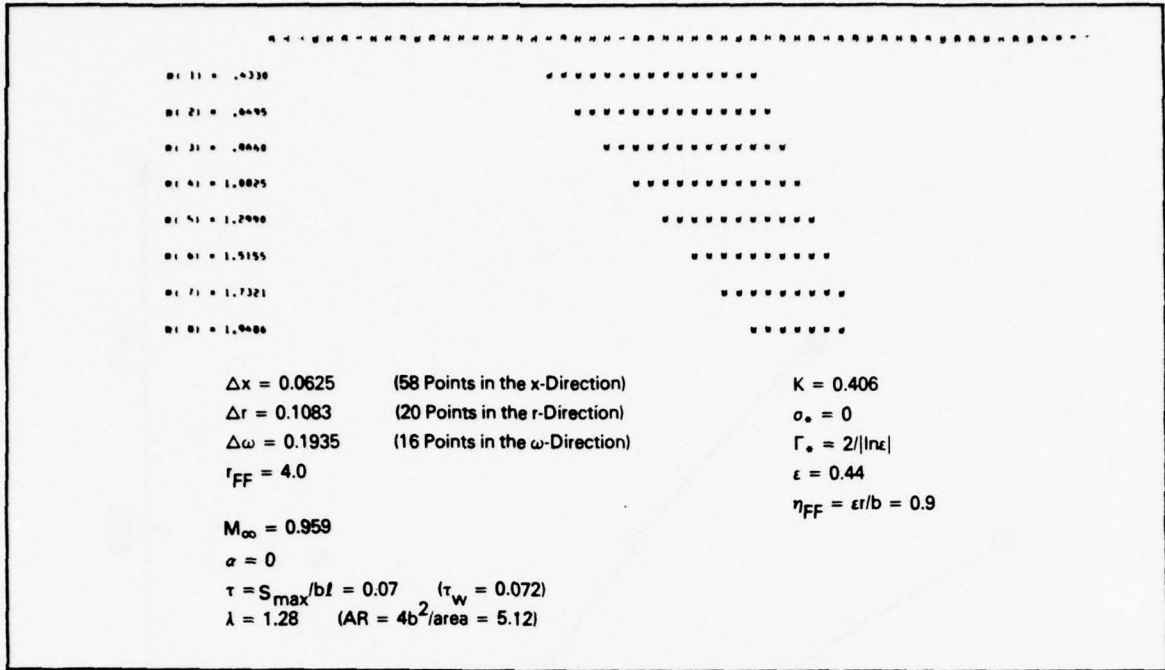


Figure 5-c. Correlation of Pressure Signatures for Wing and its Equivalent Body.

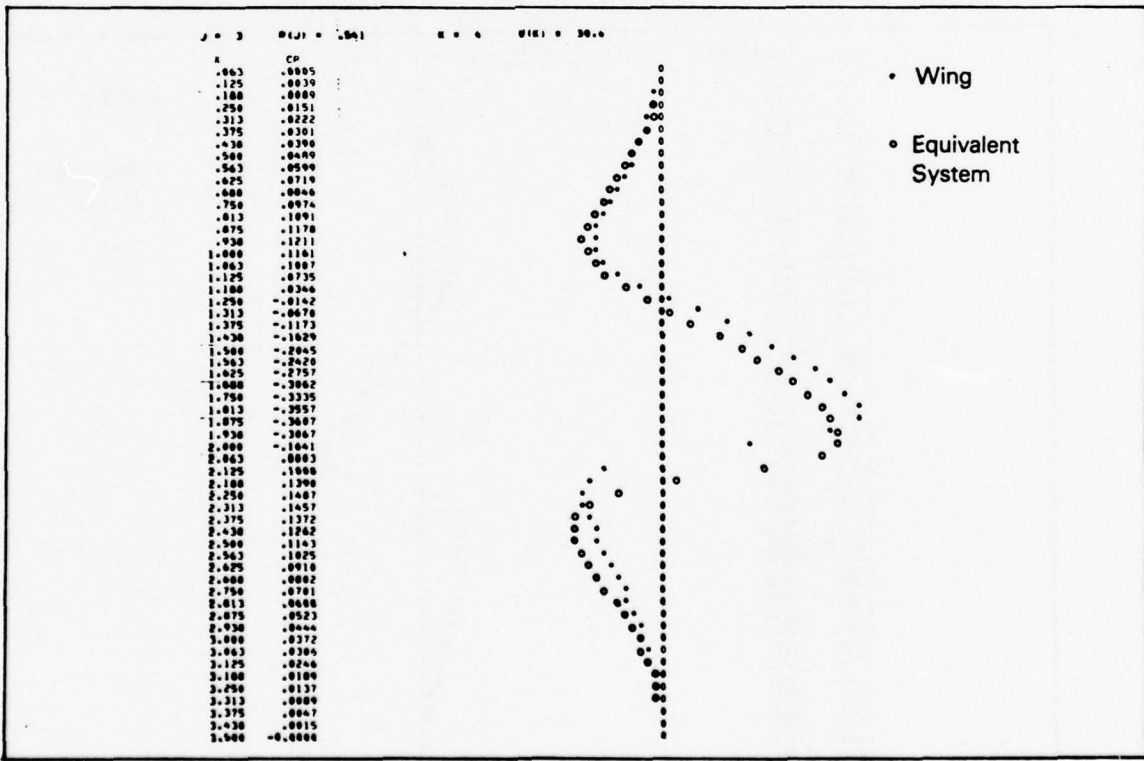
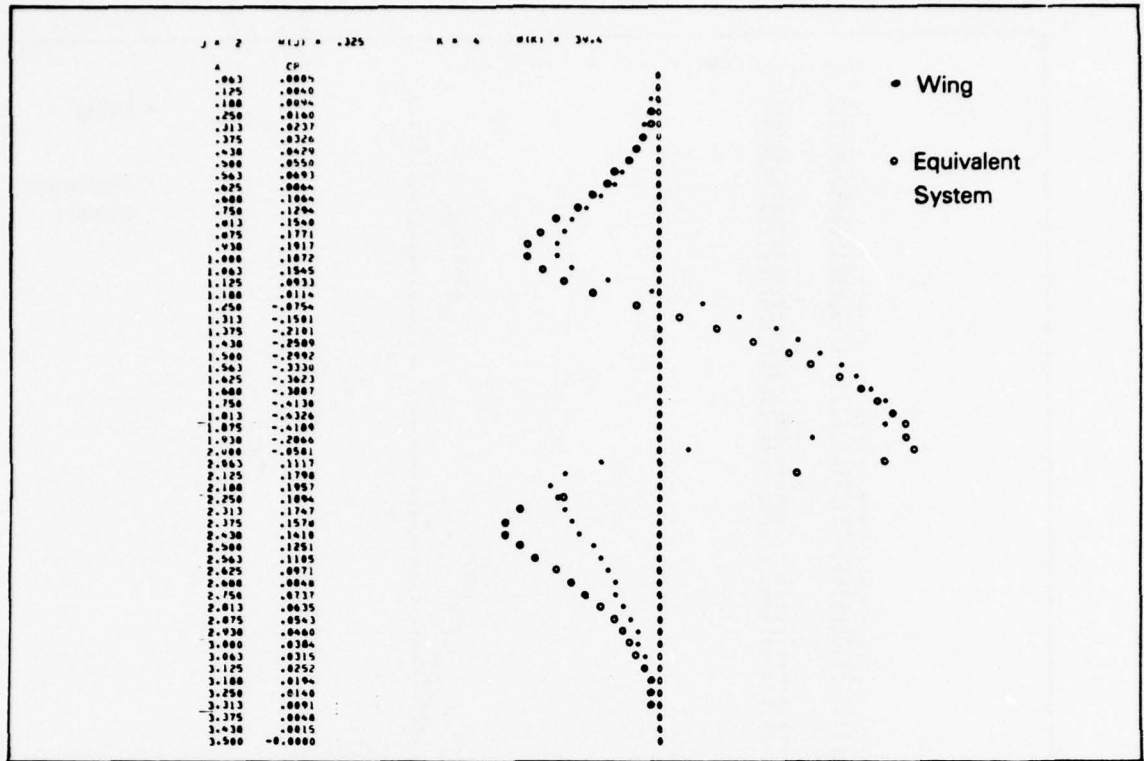


Figure 5-c. Correlation of Pressure Signatures for Wing and its Equivalent Body (Cont.)

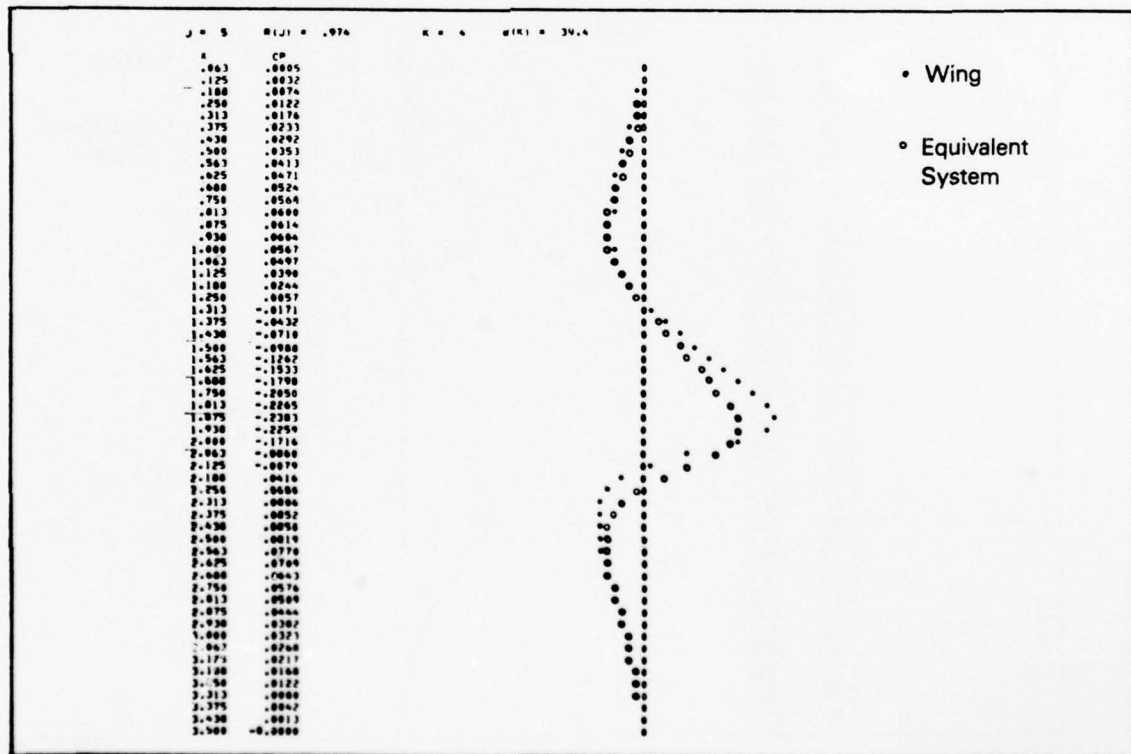
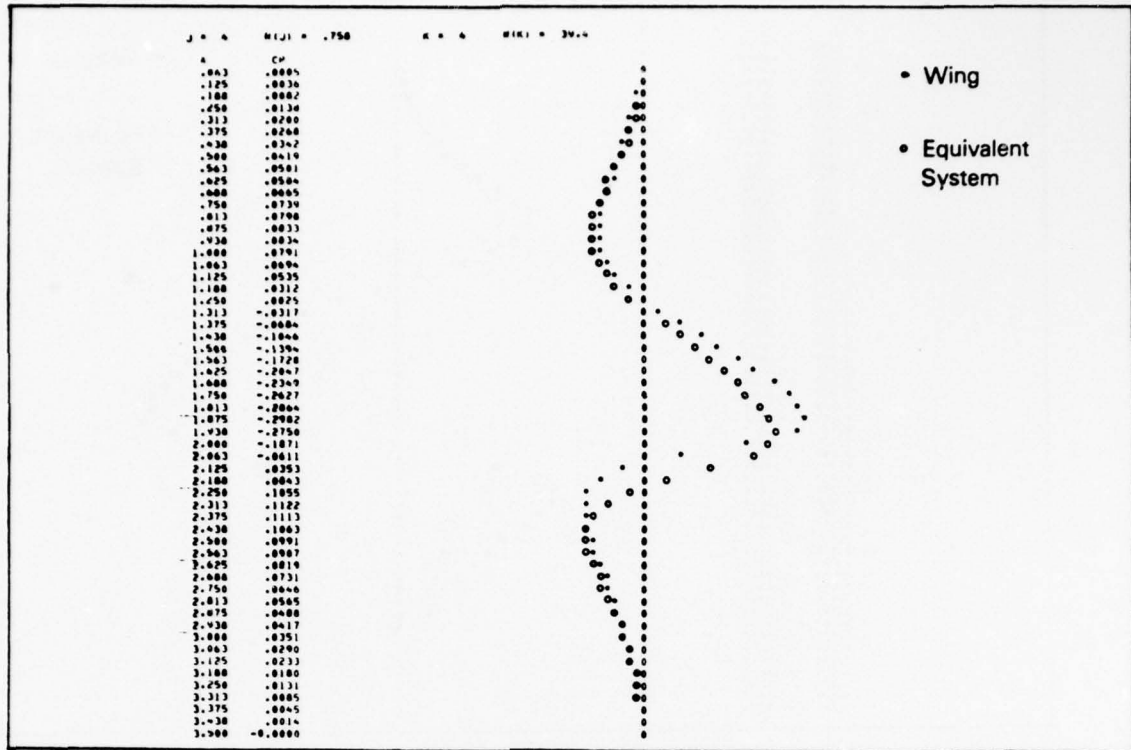


Figure 5-c. Correlation of Pressure Signatures for Wing and its Equivalent Body (Cont).

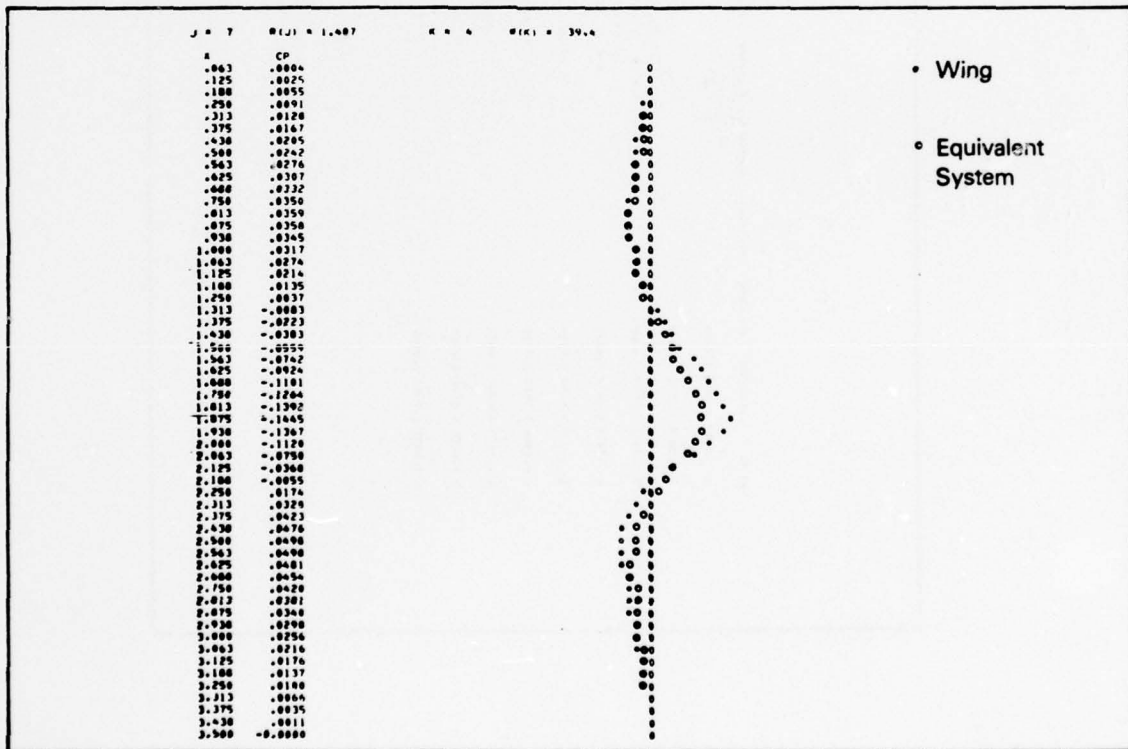
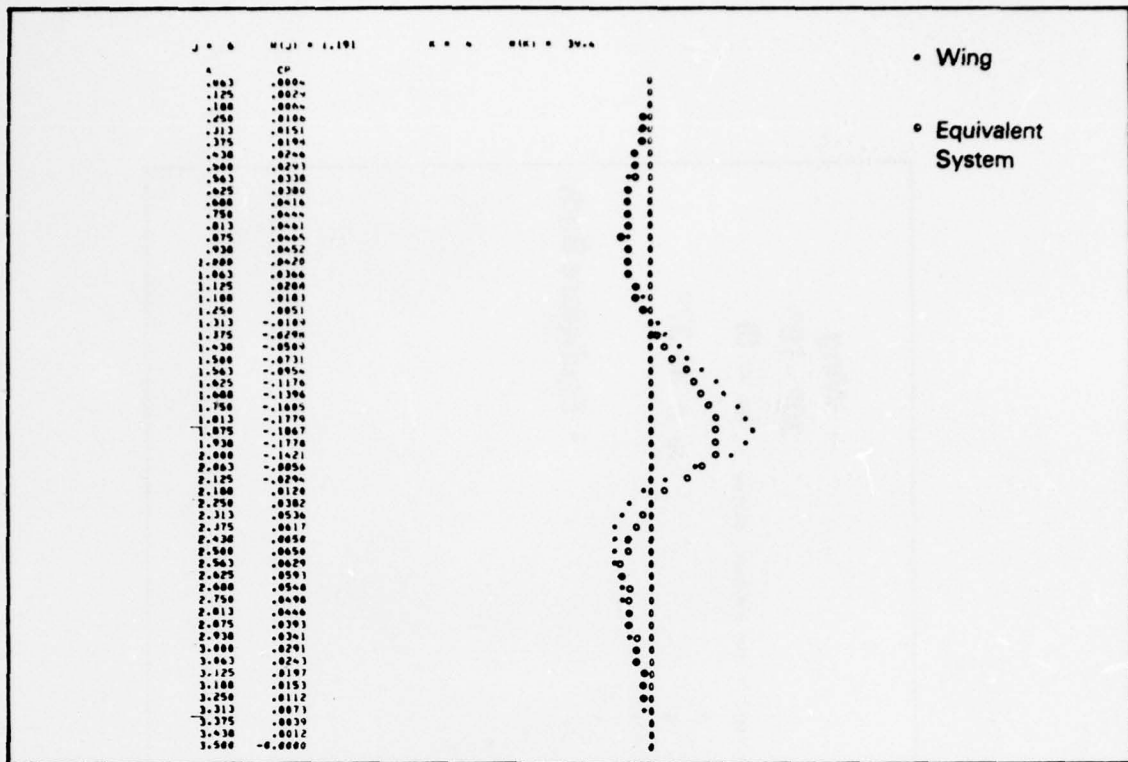


Figure 5-c. Correlation of Pressure Signatures for Wing and its Equivalent Body (Cont).

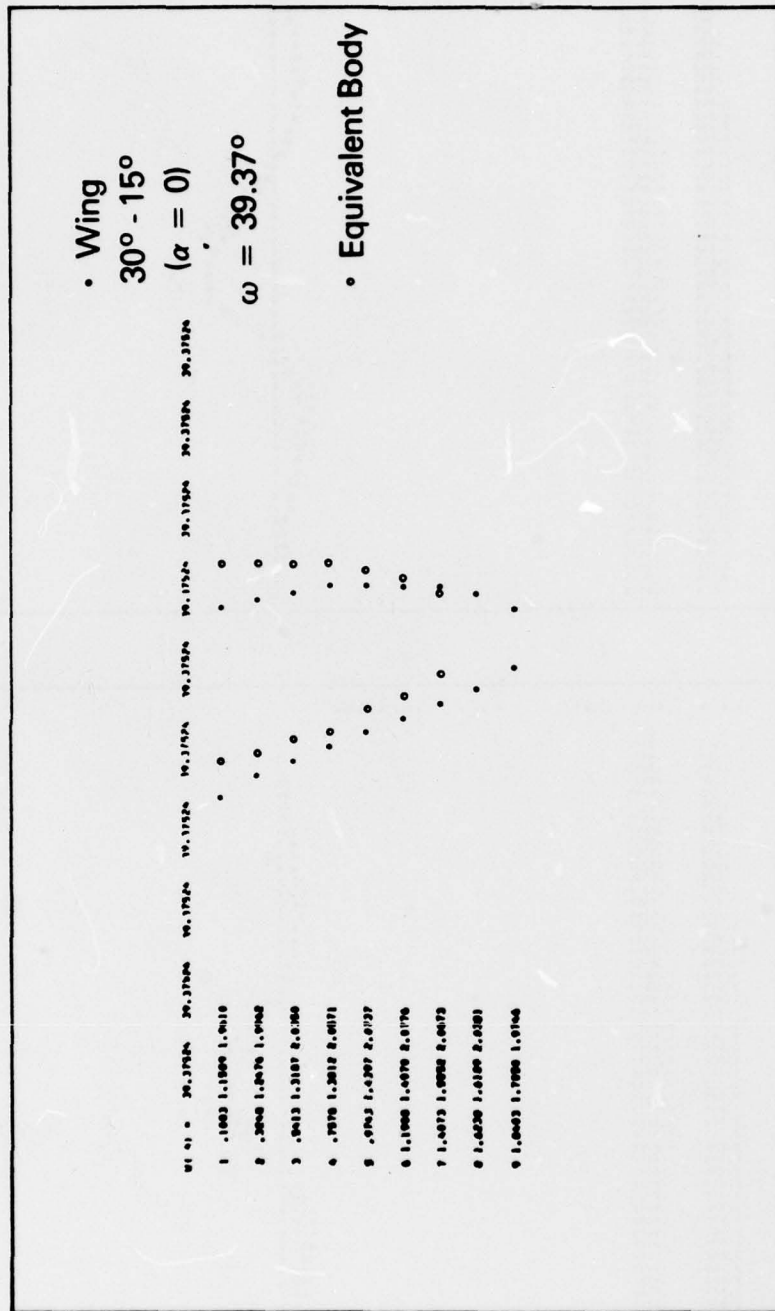


Figure 5-d. Correlation of Sonic Lines for Wing and its Equivalent Body.

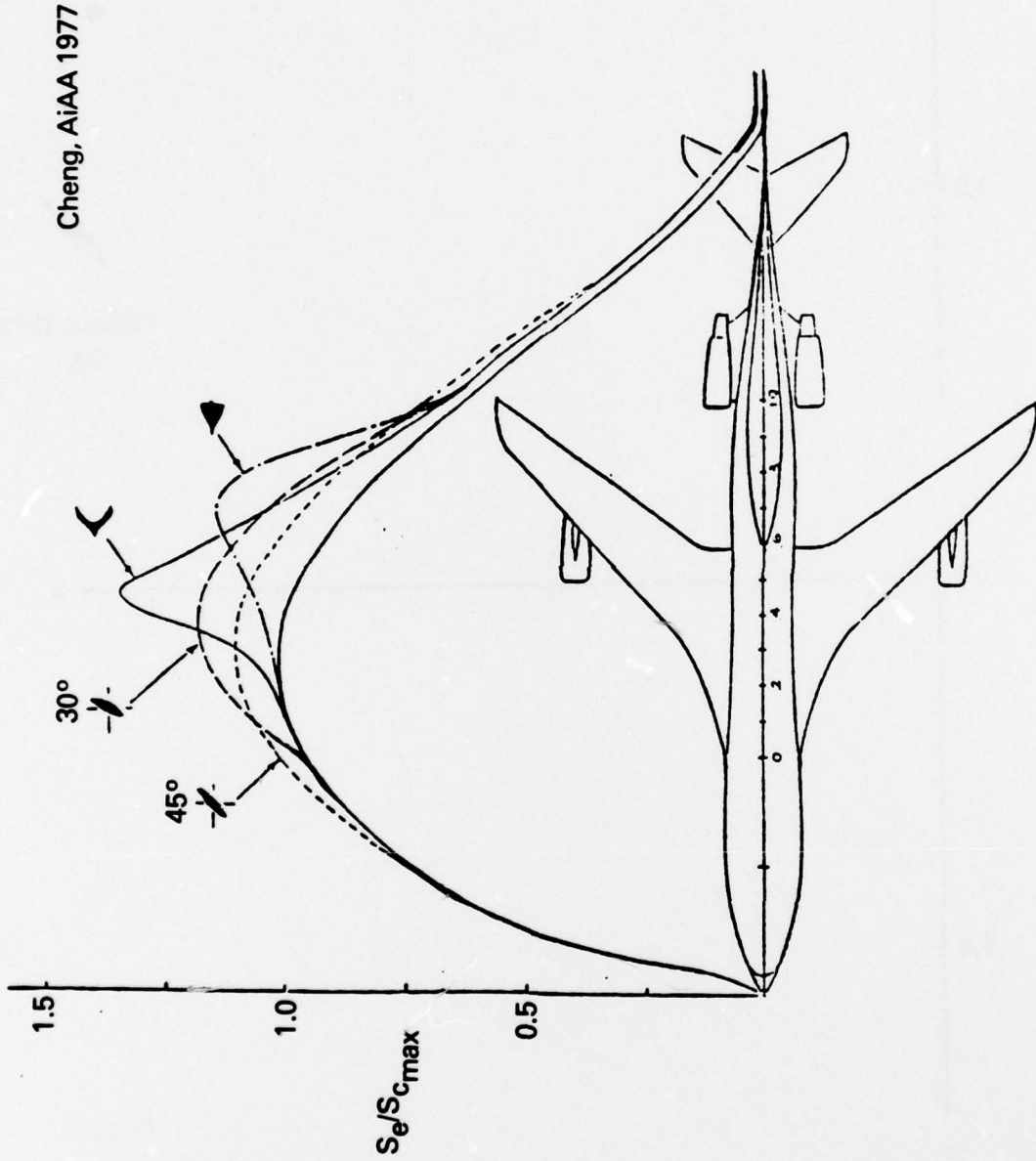


Figure 6-a. Lift Correction to Cross-Section Area Distribution.

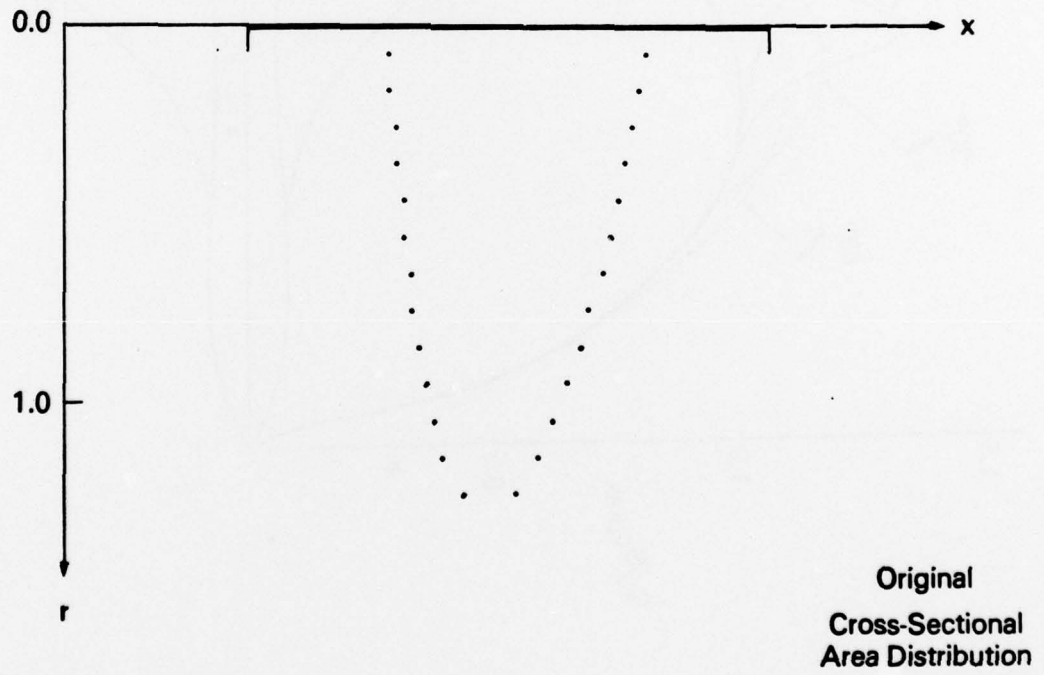
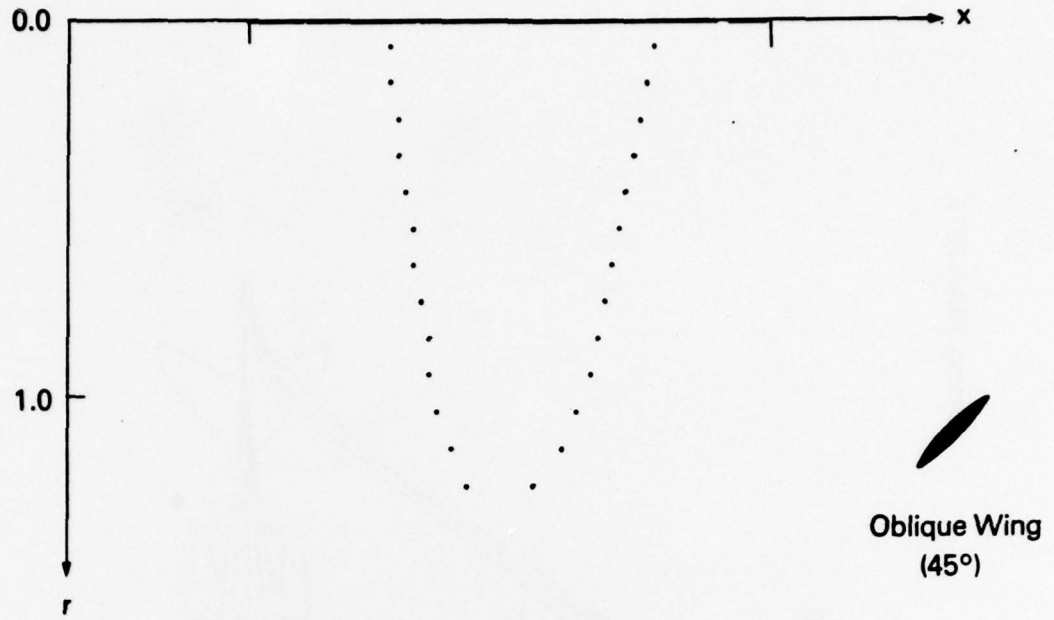


Figure 6-b. Sonic Lines of Axisymmetric Flows Around Equivalent Bodies.

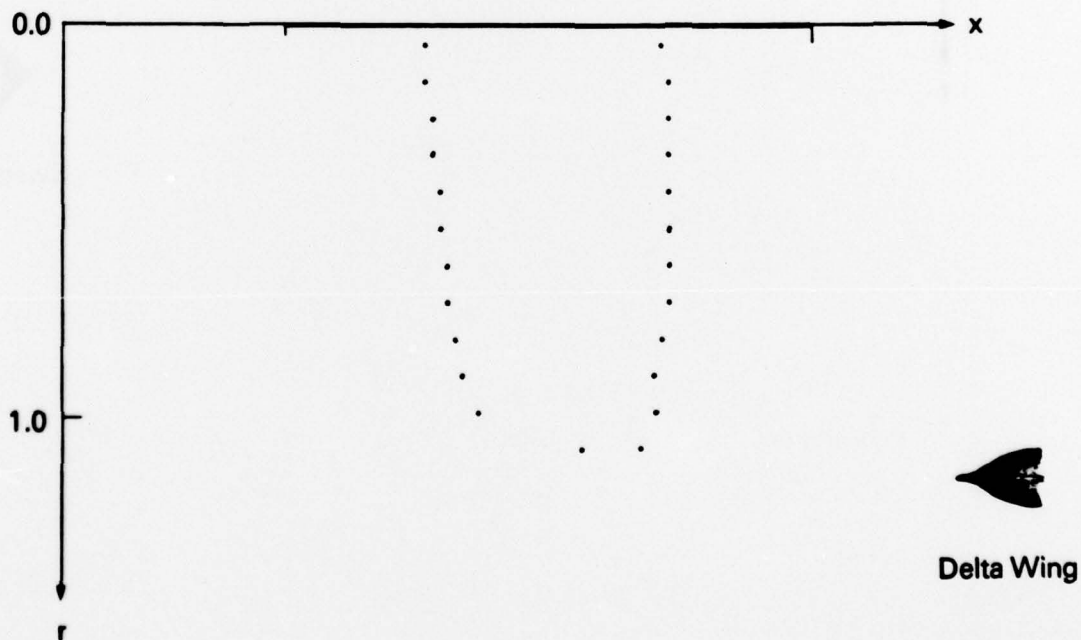
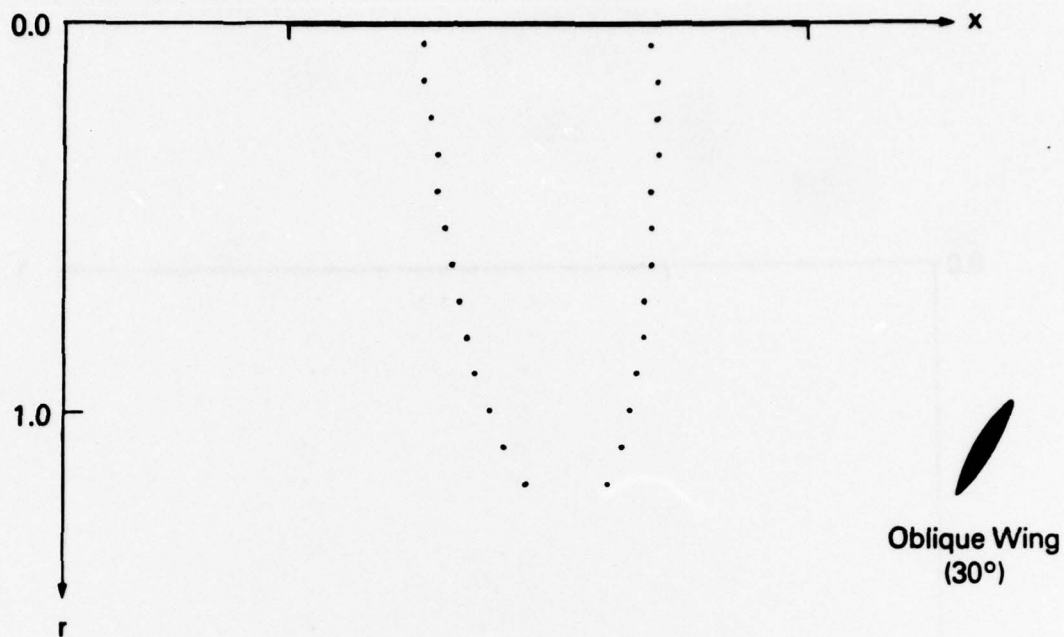


Figure 6-b. Sonic Lines of Axisymmetric Flows Around Equivalent Bodies (Cont.).

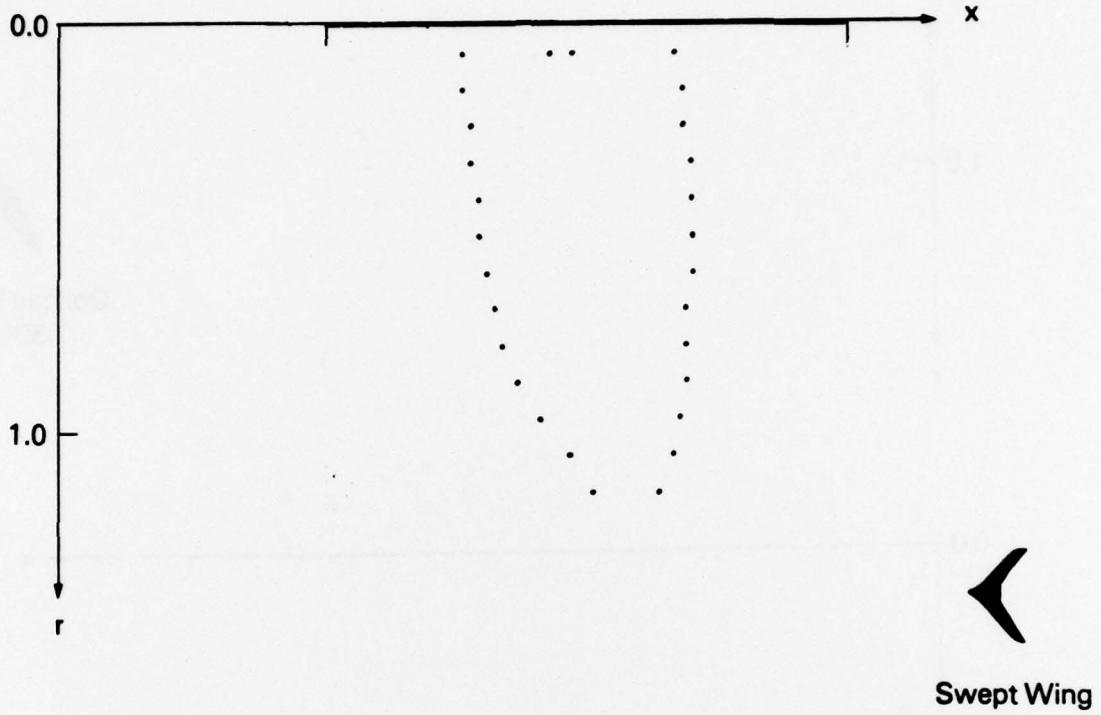


Figure 6-b. Sonic Lines of Axisymmetric Flows Around Equivalent Bodies (Cont.).

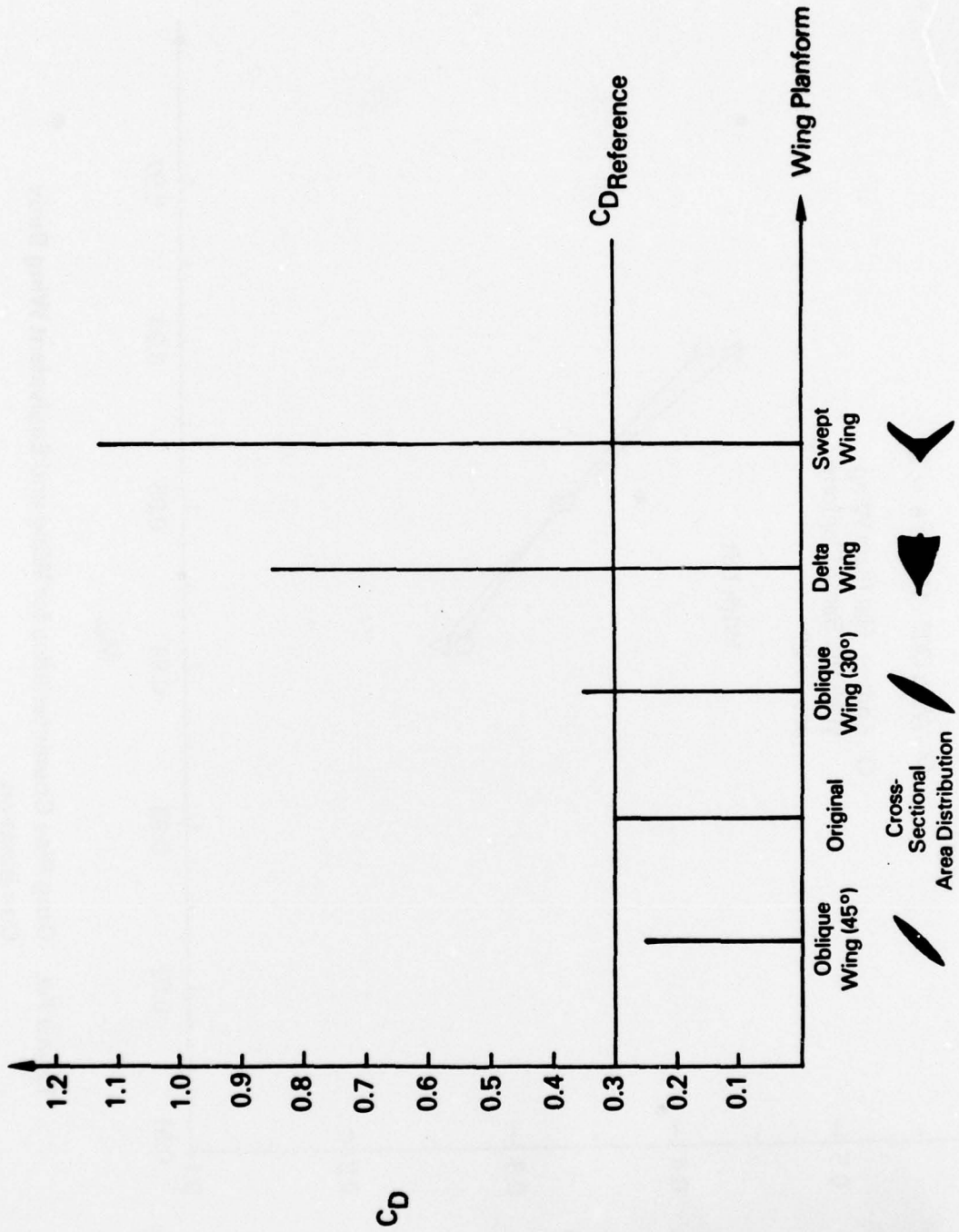


Figure 6-c. Drag Rise for Different Planforms.

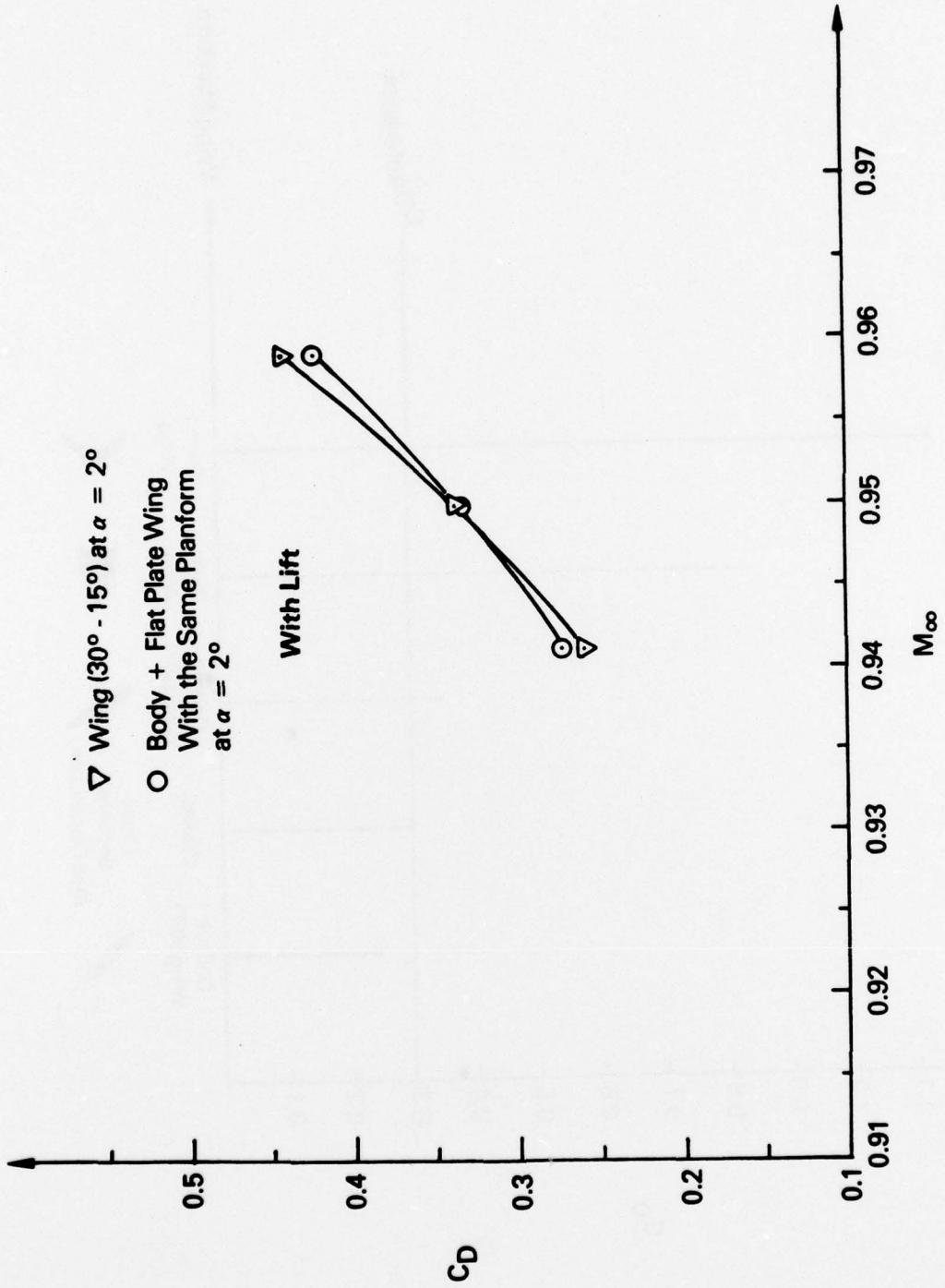


Figure 7-a. Drag Rise Characteristics for Wing and Equivalent Wing Body Combination.

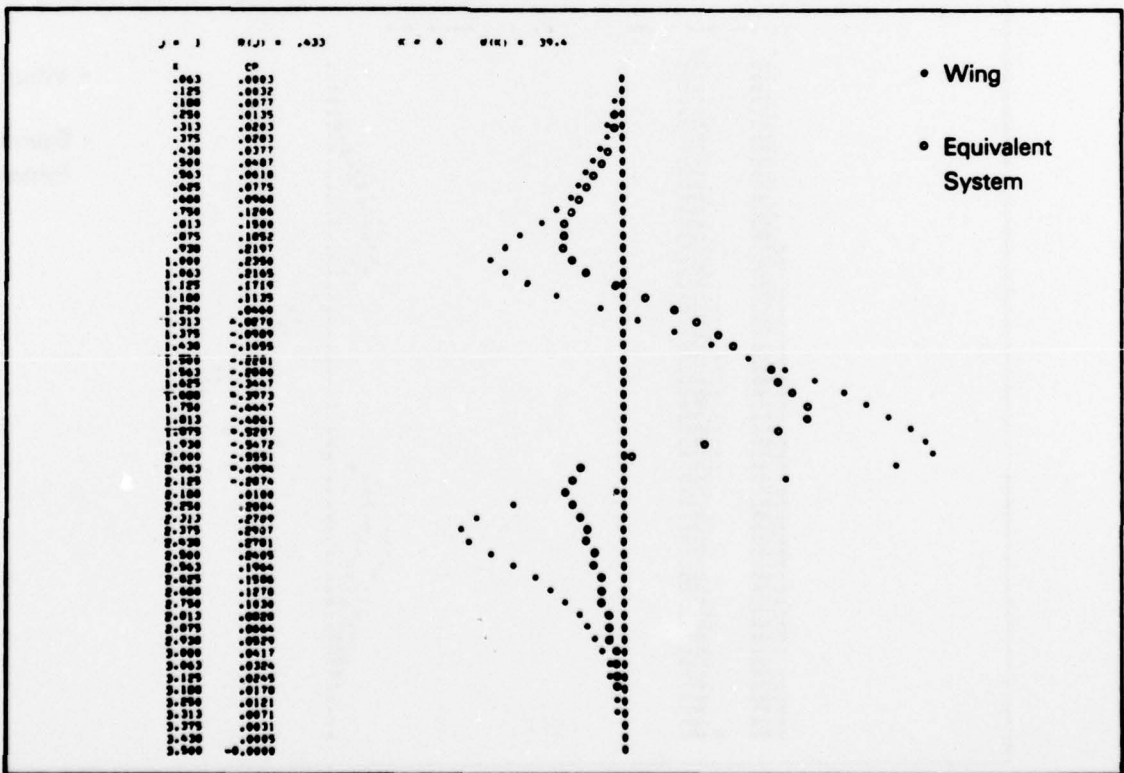
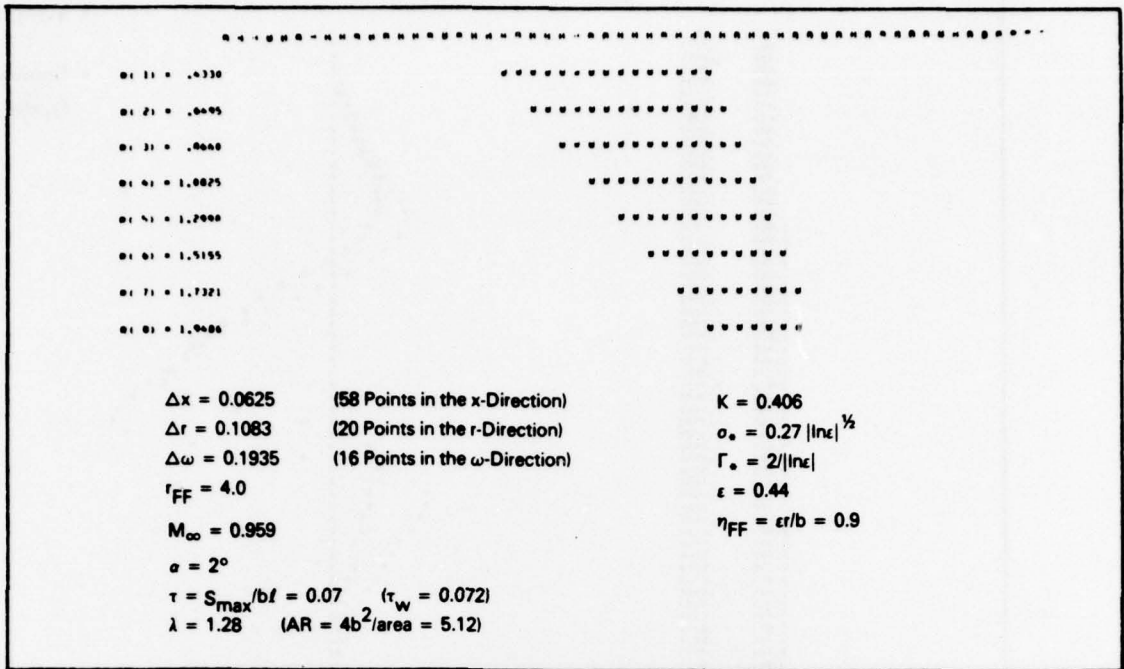


Figure 7-b. Correlation of Pressure Signatures for Wing and Its Equivalent System.

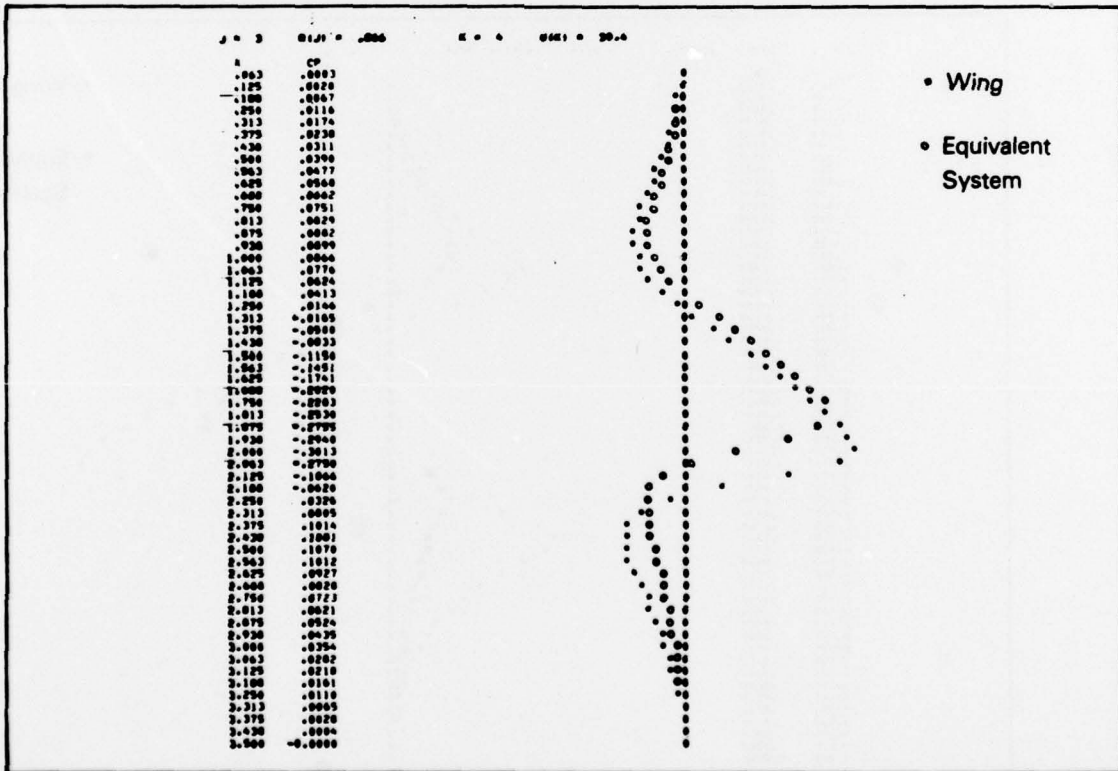
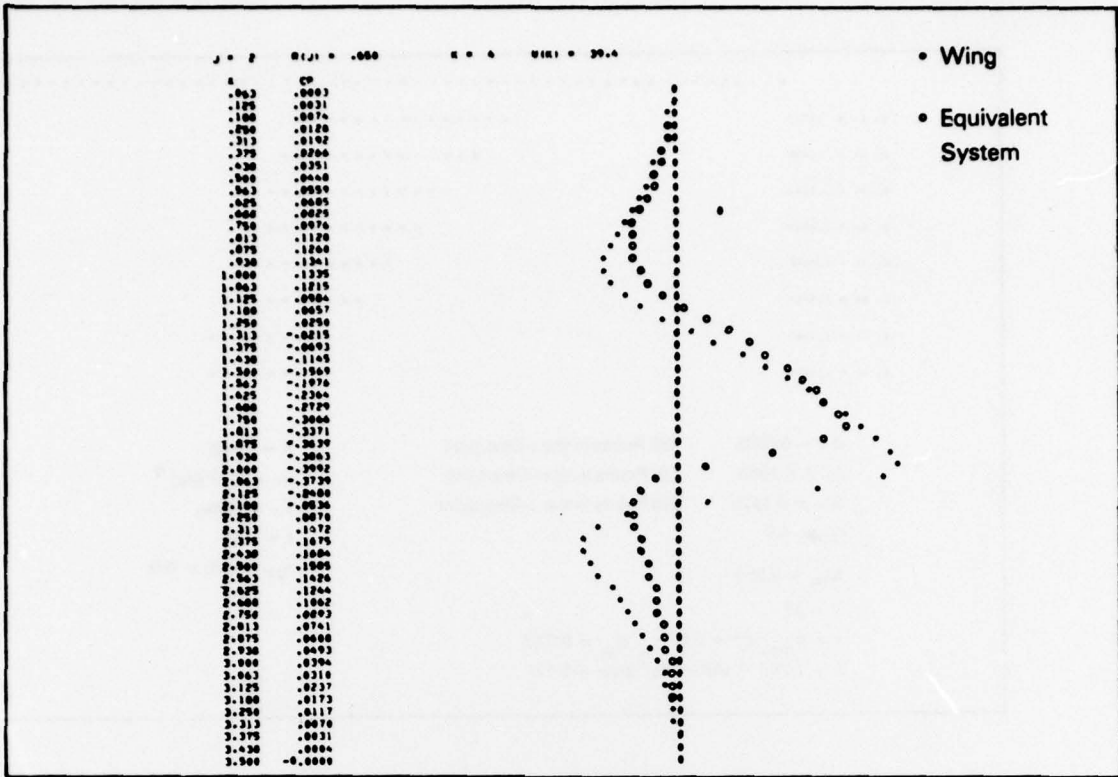


Figure 7-b. Correlation of Pressure Signatures for Wing and Its Equivalent System (Cont.).

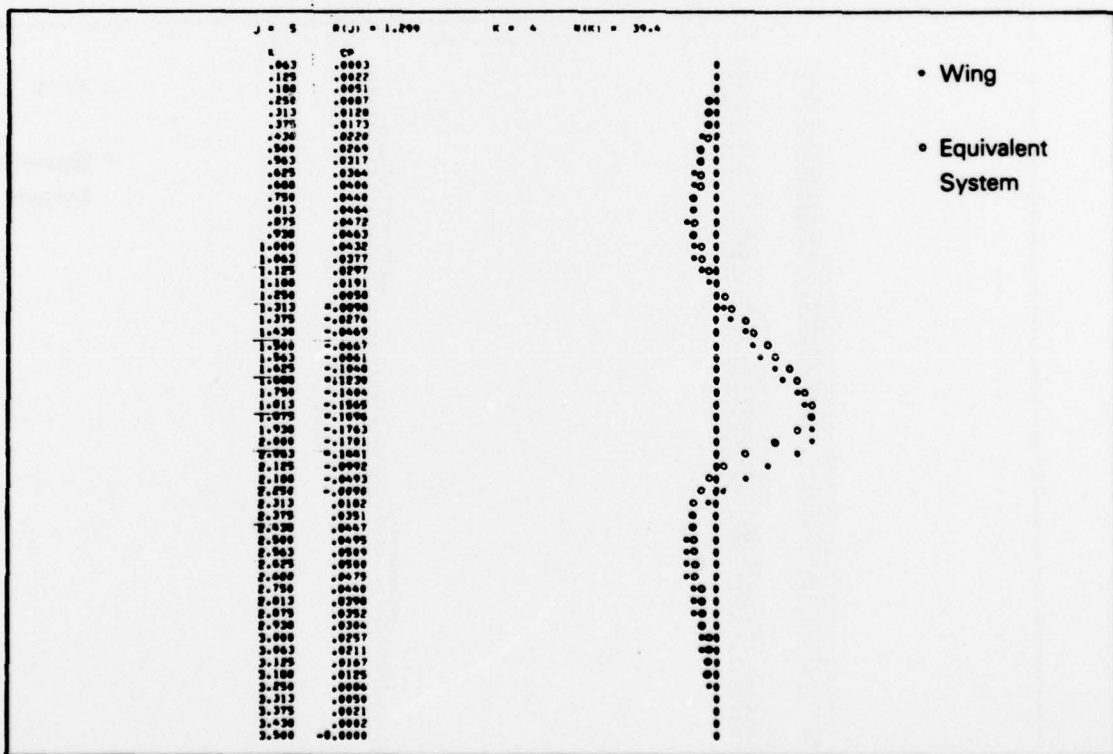
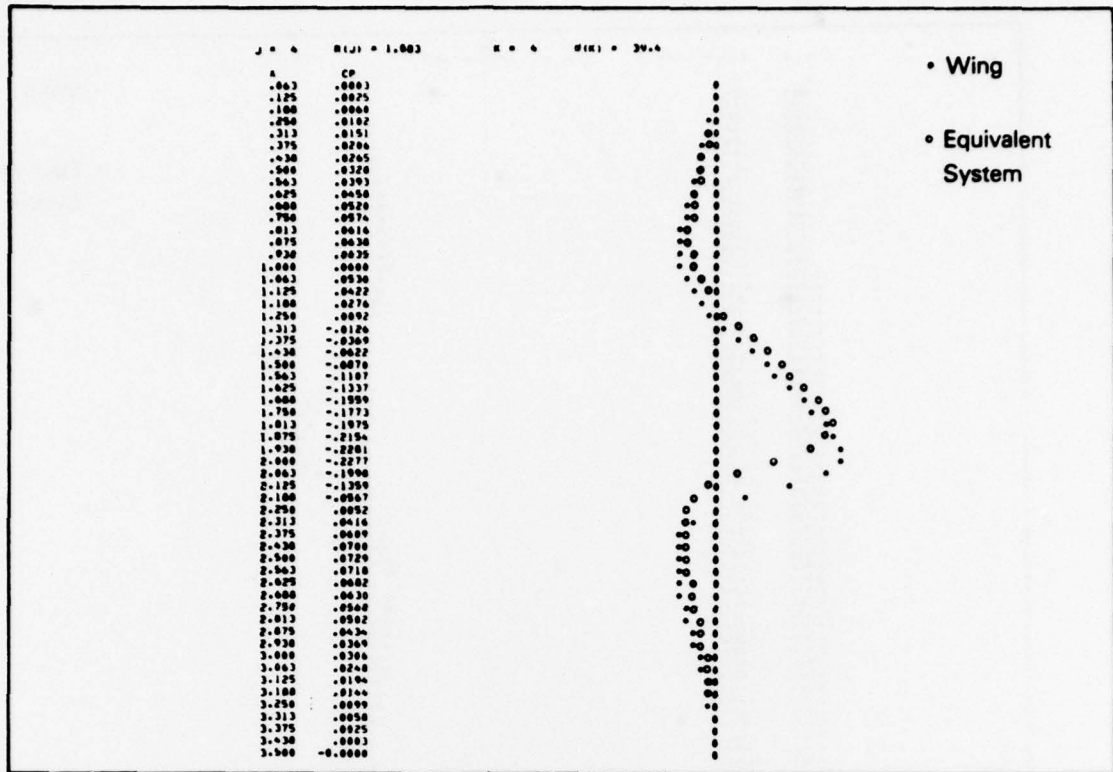


Figure 7-b. Correlation of Pressure Signatures for Wing and Its Equivalent System (Cont.).

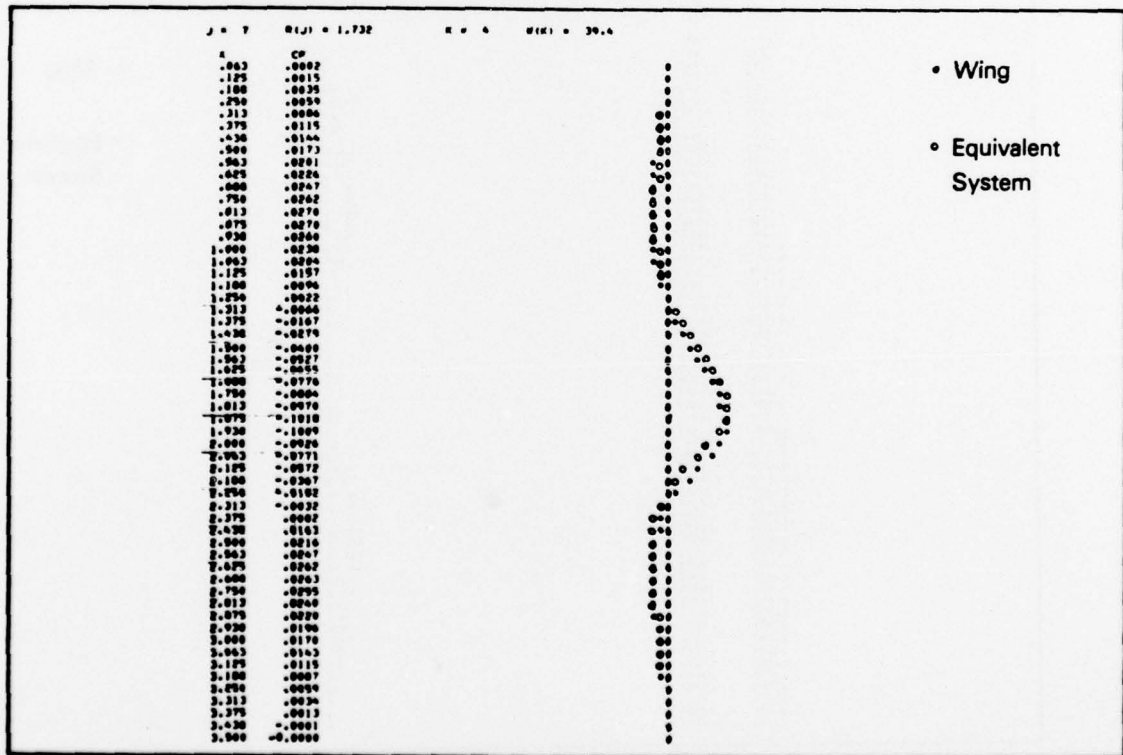
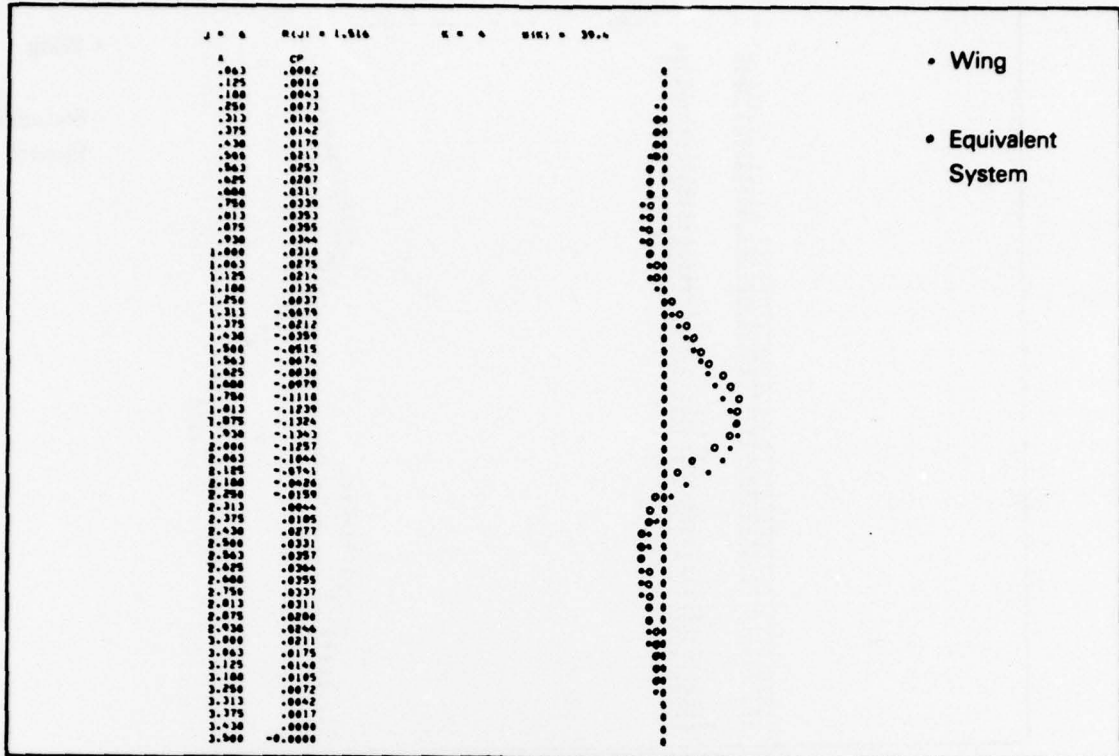


Figure 7-b. Correlation of Pressure Signatures for Wing and Its Equivalent System (Cont.).

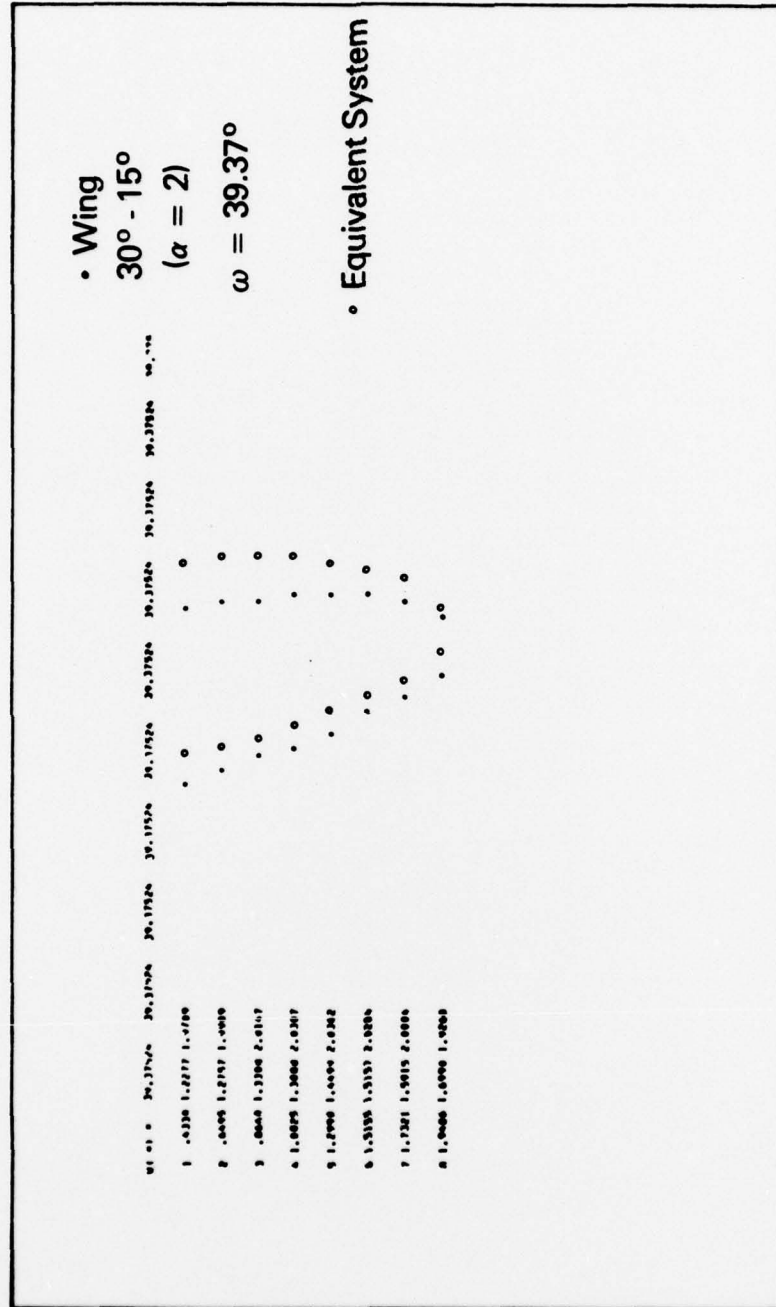


Figure 7-c. Correlation of Sonic Lines for Wing and its Equivalent System.

References

1. von Karman, T. (1947) "The Similarity Law of Transonic Flow,"
J. Math. and Phys. 26, pp. 182-190.
2. Whitcomb, R. T. (1952) "A Study of the Zero-Lift Drag Rise Characteristics of Wing Body Combination Near the Speed of Sound,"
NACA RM-L52H08.
3. Oswatitsch, K., and Keune, F. (1952) "Nichtangestellte Kortper kleiner Spannweite in Unter-und Überschallströmung," Proceedings of the Eighth International Congress of Theoretical and Applied Mechanics, Istanbul.
4. Spreiter, J. R., and Stahara, S. S. (1971) "Aerodynamics of Slender Bodies and Wing-Body Combinations at $M = 1$," AIAA Journal 9, pp. 721-730.
5. Cheng, H. K., and Hafez, M. M. (1975) "Transonic Equivalence Rule: A Nonlinear Problem Involving Lift," Journal of Fluid Mechanics 72, pp. 161-188.
6. Barnwell, R. W. (1975) "Analysis of Transonic Flow About Lifting Wing-Body Configurations," NASA TR R-440, June.
7. Cheng, H. K. (1977) "Lift Corrections to Transonic Equivalence Rule: Examples," AIAA Journal 15, pp. 366-373, March.
8. Cole, J. D. (1975) "Modern Developments in Transonic Flow," SIAM Journal of Applied Math 29, No. 4, pp. 763-787, 197.
9. Berndt, S. B. (1956) "On the Drag of Slender Bodies at Sonic Speed," The Aeronautical Inst. of Sweden, FFA Report 70.

References (Cont.)

10. Agnell, N., Mattsson, R., and Nyberg, S. E. (1978) "Investigation of the Transonic Drag Characteristics for Non-Slender Wing Body Combinations and Thin Equivalent Axisymmetric Bodies at Zero Lift," Paper presented at the 11th ICAS Congress in Lisbon, Portugal, September.
11. Cheng, H. K., and Hafez, M. M. (1973) "Equivalence Rule and Transonic Flows Involving Lift," University of Southern California, USC, AE 124.
12. Lomax, H., Bailey, F. R., and Ballhaus, W. F. (1973) "On the Numerical Simulation of Three-Dimensional Transonic Flow With Application to the C-141 Wing," NASA TN D-6933.
13. Newman, P. A., and Klunker, E. B. (1974) "Computation of Transonic Flow About Lifting Wing Cylinder Combinations," J. Aircraft 11, No. 4.
14. van der Vooren, J., Sloof, J. W., Huizing, G. H., and Van Essen, A. (1975) "Remarks on the Suitability of Various Transonic Small Perturbation Equations to Describe Three-Dimensional Flow," Symposium Transonicum II, September.
15. Schmidt, W., "A Self-Consistent Formulation of the Transonic Small Disturbance Theory," to appear.
16. Jameson, A. (1974) "Iterative Solution of Transonic Flows Over Airfoils and Wings," Comm. Pure Applied Math. 27, pp. 283-309.
17. Hafez, M. M., South, J., and Murman, M. E. (1978) "The Artificial Compressibility Methods for the Numerical Solution of the Full Potential Equation," AIAA paper 78-1148.

References (Cont.)

18. Barnwell, R. W. (1976) "Approximate Method for Calculating Transonic Flows About Lifting Wing-Body Configurations," NASA TR R-452.
19. Sedin, Y. C-J. (1978) "Qualitative Calculations of Transonic Drag-Rise Characteristics Using the Equivalence Rule," paper presented at the 11th ICAS Congress in Lisbon, Portugal, September.
20. South, J. C. (1976) "Comments on Difference Schemes for the Three Dimensional Transonic Small-Disturbance Equation for Swept Wings," NASA TM X-71980.